COMPETITION BETWEEN THE PURINE AND PYRIMIDINE TRIPLE HELIX MOTIFS IN AN OLIGONUCLEOTIDE SYSTEM

Martin Mills

Thesis presented for the Degree of

DOCTOR OF PHILOSOPHY

in the Department of Biochemistry

UNIVERSITY OF CAPE TOWN

December 1998

Abstract

Triple helices are classified into two groups according to the composition and orientation of the third strand, namely the pyrimidine motif and the purine motif. These motifs constitute two separate fields of research. It was proposed, based on the alternative design rules, that the two motifs can in fact lead to competing structures. An oligonucleotide system has been designed to demonstrate this competition. Systematic variation of it's components give insight into the requirements for optimal binding of a third strand.

A palindromic, homopyrimidine oligonucleotide of 22 bases was designed to form an overlapping 9-base, Watson-Crick (WC), duplex with a partly complementary 22-base purine-rich oligonucleotide. This leaves two free 3′ extensions under conditions when only the duplex is stable. If the conditions, however, favour triplex formation the pyrimidine tail can compete with the purine-rich tail as third strand for the duplex forming Hoogsteen or reverse-Hoogsteen hydrogen bonding respectively with the purines in the WC double strand. The underlying triplexes and core duplex were synthesised and characterised as controls.

The technique of UV-melting was used to establish phase diagrams (T_m vs pH) to characterise the boundary conditions under which each construct is stable. The effect of pH, counterions, sequence composition and mutations (local base exchange) were evaluated from a comparison of the melting temperatures and the behaviour of the

phase boundaries. The technique of gel-retardation electrophoresis was used to distinguish the duplex from the control purine triplex.

This thesis shows that the purine and pyrimidine motifs can compete for the same purine strand of the core double helix and can be converted into each other by just change in pH in the presence of magnesium ions. By systematically replacing thymine with adenine within the reverse-Hoogsteen strand a linear increase in the stability (T_m) of the purine motif is observed. The following trend arises for the increase in stability of the purine motif, listing the most to least preferred triads:

A-AT > T-AT = I-AT > C-AT where C is considered a mismatch.

These results allow one to specify the rules required for a rational approach to the design of oligonucleotide third strands.

Acknowledgements

When asked what I am researching I safely say, "I study unusual DNA structures".

I am indebted to my supervisor Prof. Horst Klump for showing me that DNA is not just a long, monotonous, two dimensional data base, but a truly flexible molecule capable of forming double, triple and quadruple stranded structures as well as hairpins, pseudoknots, three and four-way junctions and even cubes.

Triple helical structures, in particular, have a potential role in regulation of gene expression and triplex studies are showing promise for therapeutic application conventionally called "gene therapy". Thoroughly motivated to be a part of the research effort I was given a flying start with a most elegant system for my Honours project and excellent supervision by Dr. Jens Völker. Now five years later, with guidance from Prof. Klump and Dr. Paul Hüsler the system has evolved to yet another unusual structure which gives insight into the triple helix and the flexibility of nucleic acid conformations.

Many thanks for the support of my colleagues Madhu Chauhan, Neo Makube, Renate Petry and William Adonis. I gratefully acknowledge the invaluble input of the thesis referees, Prof. Kenneth Breslauer, Prof. Juli Feigon and Dr. Jean-Louis Mergny and the financial support of the Molecular Biology Department, the University Research Council (URC) and the South African Foundation for Research Development (FRD).

Thank you Penelope and Robin Mills for your support in everything.

Dedication

A.M.D.G. This thesis is dedicated to

Morris and Daisy Mills and Jack and Moira Howman.

"I have a little shadow that goes in and out with me,
And what can be the use of him is more than I can see.
He is very, very like me from the heels up to the head;
And I see him jump before me, when I jump into my bed.
The funniest thing about him is the way he likes to grow,
Not at all like proper children, which is always very slow;
For he sometimes shoots up taller like an india-rubber ball,
And he sometimes gets so little that there's none of him at all.
He hasn't got a notion of how children ought to play,
And can only make a fool of me in every sort of way.
He stays so close beside me, he's a coward, you can see;
I'd think shame to stick to nursie as that shadow sticks to me!
One morning, very early, before the sun was up,
I rose and found the shining dew on every buttercup;
But my lazy little shadow, like an arrant sleepy-head,
Had stayed at home behind me and was fast asleep in bed."

My Shadow by Robert Louis Stevenson

"Give me a word,
Give me a sign,
Tell me where to look,
Tell me what will I find."

(Prayer of a researcher?) *Shine by Collective Soul*

"In the beginning...there was phosphate chemistry." *Martin Mills*

Table of Contents

Figures & Tables

Figures

Tables

Abbreviations

A	Adenine
T	Thymine
G	Guanine
C	Cytosine
U	Uracil
I	Inosine (Hypoxanthine)
CD	Circular Dichroism
DNA	Deoxyribonucleic acid
DTT	Dithiothreitol
EDTA	Ethylenediaminetetraacetic acid
FTIR	Fourier transform infrared spectroscopy
Na^+	Sodium cation
$[Na^+]$	Molar concentration of sodium cations
NMR	Nuclear Magnetic Resonance
PAGE	Polyacrylamide gel electrophoresis
HG	Hoogsteen
RHG	Reverse-Hoogsteen
RNA	Ribonucleic acid
UV	Ultra-violet
WC	Watson-Crick

Introduction

1.1 Discovery of a three stranded helix made up of polynucleotides

1.1.1 Polynucleotides form triple helical structures

It was not long after the discovery of the DNA double helix (Watson & Crick, 1953) that an analogous double helix of RNA was reported formed by poly r(A) and poly r(U) (Warner, 1957). It fell to Alexander Rich, David Davis and Gary Felsenfeld to discover a triple stranded structure while creating a UV-mixing curve with these ribopolynucleotides. Two strands of poly r(U) combine in the presence of 10 mM magnesium ions with one strand of poly r(A) to form poly r(U).poly r(A).poly r(U) (Felsenfeld *et al.*, 1957). Investigation by X-ray diffraction of fibres revealed a third strand wrapped in the major groove of the double helix bound to the underlying purine strand (Rich, 1958).

Within two years Hoogsteen reported an alternate base-pairing scheme to that of Watson and Crick between 9-methyladenine and 1-methylthymine and it became a proposed scheme for attaching a third base to the purine in a canonical WC double helix (Hoogsteen, 1959). This alternate scheme was confirmed with infrared data showing hydrogen bonding of atoms N_6 and N_7 of Adenine with O_6 and N_1 of Uracil in poly (U-AU) (Miles, 1964). Binding of a third strand is now referred to as Hoogsteen- (HG) or Reverse-Hoogsteen (RHG) hydrogen bonding depending on the orientation of the third strand i.e. parallel or antiparallel to the WC purine strand. The nucleotide in the third strand is usually written first followed by the purine of the duplex, to which it is bound, followed by the complementary pyrimidine e.g. poly (U-AU).

Analogous to poly (U-AU) a triplex of poly (I-AI) was reported. This shows how easily a third strand is accommodated in the major groove as the diameter of the poly (I-AI) triplex is 27.7 Å which is very close to 23.2 Å of normal A'-RNA double helix (Arnott & Selsing, 1974). Inosine or hypoxanthine can be involved in the following triplexes under physiological conditions: poly (I-AU) and poly (I-GC) (Letai *et al.*, 1988) contain poly I as the Hoogsteen (HG) strand, poly (C^+-IC) (Thielle & Guschlbauer, 1968) contains it as one of the WC strands and in poly (I-IC) (Fresco & Masoulie, 1963) the inosine serves as the HG and a purine WC strand respectively. This created the impression that inosine can substitute either U, T and C or G in the Hoogsteen position.

Fundamental research into mixtures of other polynucleotides revealed new DNA triplexes such as poly (T-AT) (Arnott & Selsing, 1974), poly(G-GC) (Mark & Thiele, 1978) at neutral pH and poly (C^+- GC) (Lipset, 1964) on protonation of cytosine at low pH. In all these triplexes the third strand bases hydrogen-bond with the purine bases of the duplex. This binding pattern is preferred over binding to the pyrimidine bases as purines can form two HG hydrogen bonds in addition to the canonical WC hydrogen bonds while the pyrimidines can only form one. It was shown that triplexes are not formed on alternating purine-pyrimidine sequences (Morgan & Wells 1968). Severe backbone distortion would arise if the third-strand bases would switch consecutively from one strand of the duplex to the other. The precondition for triplex formation is therefore a homopurine/homopyrimidine tract in a WC double helix to which the third strand can attach itself.

Both pyrimidine and purine bases can form two hydrogen bonds with the purine strand of the duplex and two main classes of triple helix arise called the pyrimidine- and purine-motifs respectively. Models of the base-pairing schemes are shown in Figs. 1.1a and 1.1b.

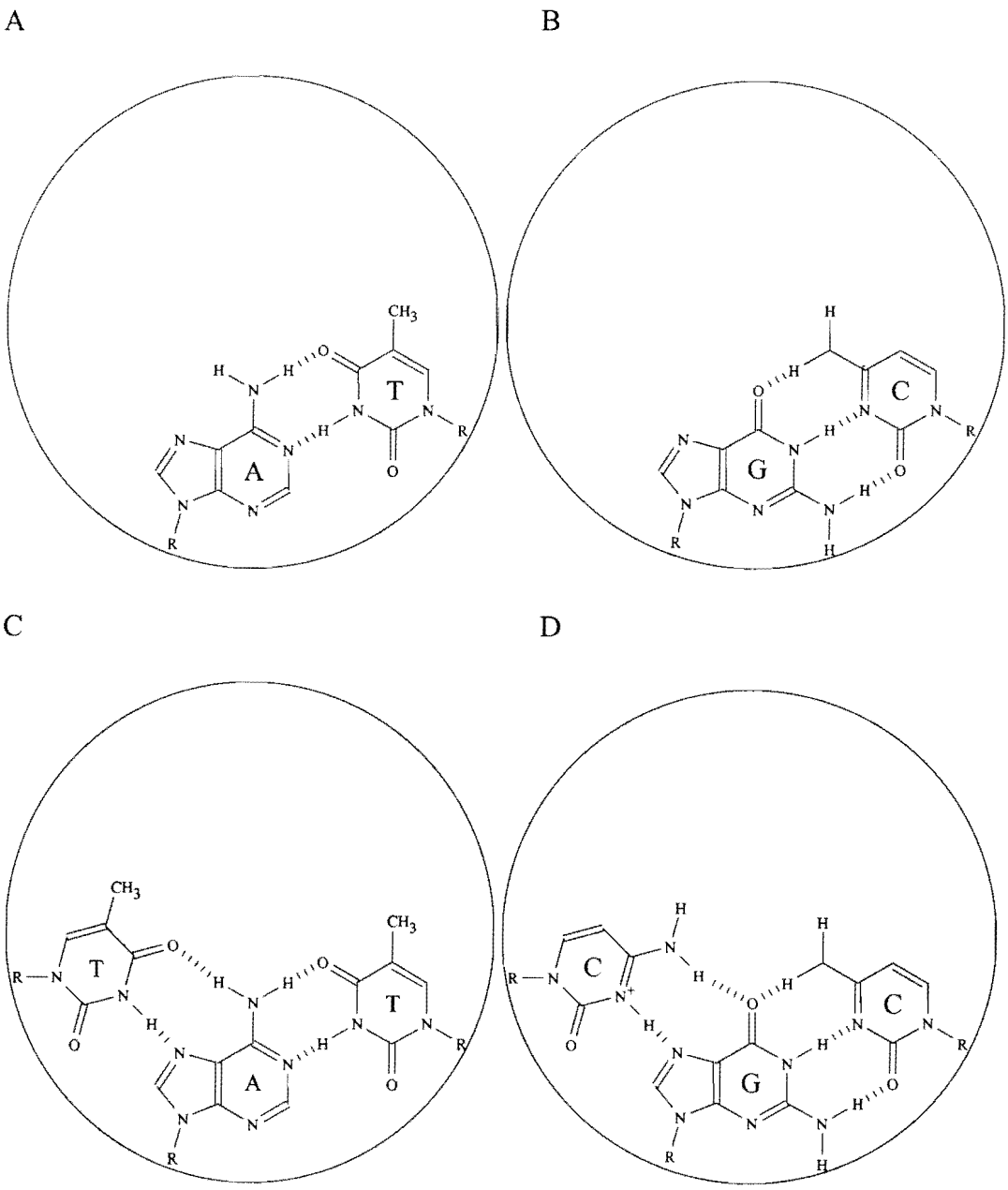

Fig. 1.1a. Models of Watson-Crick basepairs and canonical Hoogsteen base triplets:

A) A·T Watson-Crick basepair; B) C·G Watson-Crick basepair

C) T-A·T Hoogsteen triplet; D) C^+-G·C Hoogsteen triplet

A

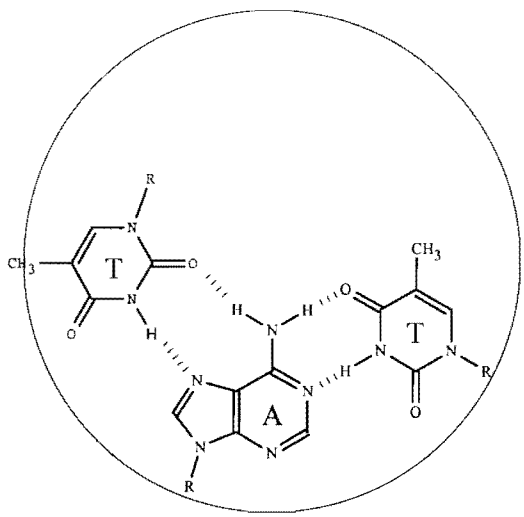

B

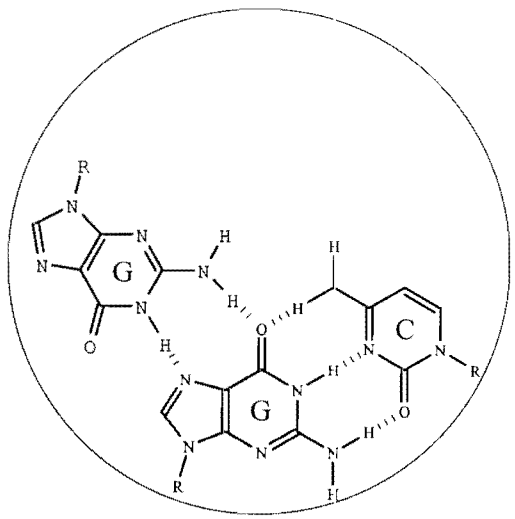

C

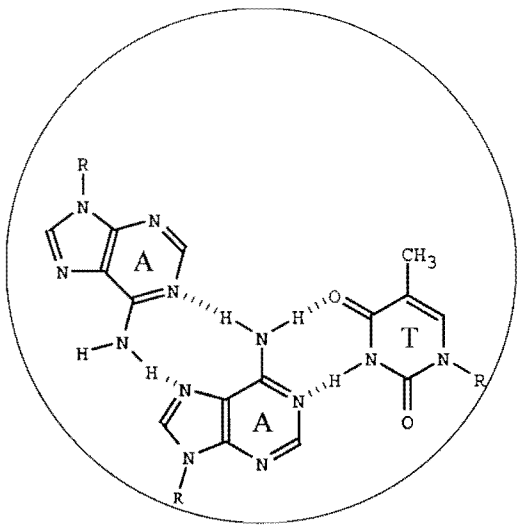

Fig. 1.1b. Models of Reverse-Hoogsteen base triplets:

A) T-A·T

B) G-G·C

C) A-A·T

1.1.2 Triple helical structures found in natural DNA

Triplex research has a long history and the early work on polynucleotides laid the foundation for an understanding of the general properties of triple helices. Triplex formation is restricted to homopurine-homopyrimidine tracts in the WC-double helix but can accommodate either homopurine or homopyrimidine third strands which may have ribose or deoxyribose in their backbones.

Initial interest in the polynucleotide-based triple helix waned as the structures were considered unusual properties of polynucleotides with no biological significance. It was only in the mid 1980's that it was recognised that a triplex can form within purine-pyrimidine tracts in naturally occurring DNA of plasmids under the influence of superhelicity (Lyamichev et al., 1986). The structure called H-DNA forms when a palindromic homopurine-homopyrimidine insert in the WC duplex separates and half of the pyrimidine strand folds back onto the duplex to form a triple helix while the complementary purine sequence remains single stranded. Recent evidence suggests that this structure may play a role in DNA replication and transcription (review Mirkin & Frank-Kamenetski, 1994). With the advent of automated DNA synthesis one could model this system using oligonucleotides and triplex research entered a more applied phase.

1.2 Triplex Technology

1.2.1 Triple helix forming oligonucleotides

In 1987 two laboratories showed by elegant means that oligonucleotides can form sequence-specific triples helices with a target duplex. Heinz Moser and Peter Dervan of the California Institute of Technology presented a triple-helix-forming oligonucleotide (TFO) with an Fe-EDTA moiety covalently attached (Fig. 1.2). The oligonucleotide provides the recognition through sequence specificity and the chemical attachment provides the cleavage of the duplex by free radical formation on addition of DTT. The construct acts as an artificial restriction enzyme (Moser & Dervan, 1987). At the same time a group, headed by Claude Hélène, at the Natural History Museum in Paris reported recognition, photo-crosslinking and cleavage of duplex DNA with an oligonucleotide with an intercalating group attached (Le Doan et al., 1987; review Hélène et al., 1989). The laboratories of Dervan and Hélène remain in intense competition to this day and have driven the field forward through innovative approaches (review Chan & Glazer, 1997).

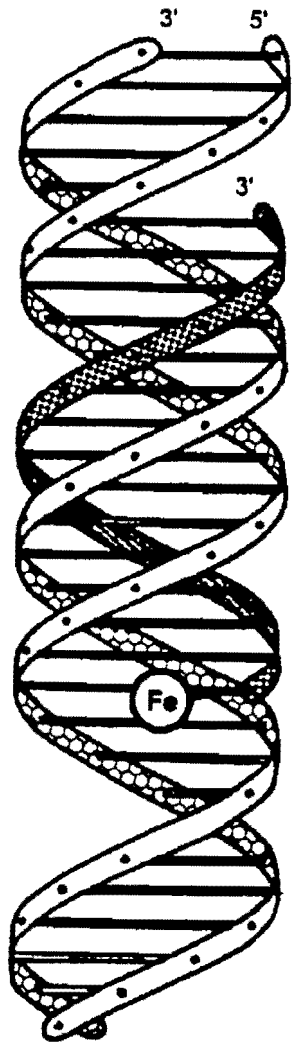

Fig. 1.2 A schematic model of an artificial restriction enzyme based on a triple helix forming oligonucleotide (Moser & Dervan, 1987).

The most tantalising application then demonstrated was that an oligonucleotide bound to a DNA double strand could repress transcription of the human *c-myc* gene in vitro (Cooney et al., 1988). The concept of inhibiting the expression of disease causing genes by targeting the DNA duplex with a third strand and supressing transcription is an elegant one. It is termed Triplex Technology or Antigene Technology as opposed to Antisense Technology (Hélène et al., 1992). The antisense approach involves sequestering the mRNA of the target gene by administering an oligonucleotide with complementary sequence to the single stranded RNA which forms a duplex by simple WC base pairing (Uhlmann & Peyman, 1990). The chimera is conveniently cleaved by the ubiquitous enzyme RNase H with some efficiency and thus inhibits translation (Kandimalla & Agrawal, 1994).

Triplex technology, on the other hand, aims at the DNA itself and is therefore more appealing from a therapeutic and thermodynamic point of view as one need not target multiple copies of mRNA thus reducing the oligonucleotide concentration required. Table 1.2 contains a list of genes (compiled from reports up to 1995) to which the triplex approach has been applied. Promises of a gene therapy are premature as many pharmacological aspects have yet to be studied and a fundamental understanding of oligonucleotide binding is a prerequisite.

TFO's have shown high affinity to a target site within a mammalian gene (Vasquez et al., 1995) and even single-site specificity within a yeast chromosome (Ströbel & Dervan, 1990). Inhibition of Rous Sarcoma Virus replication and cell transformation has been demonstrated with TFO's (Zamecnik & Stephenson, 1978), as well as

inhibition of restriction endonuclease cleavage (François et al., 1989) and binding of some DNA-binding proteins (Maher et al., 1989). TFO's find many practical applications (ex. Soyfer & Potamen, 1996):

1. Extraction and purification of specific nucleotides
   a. Triplex affinity capture (Ito et al., 1992a-c)
   b. Affinity chromatography (Pei et al., 1991; Kiyama et al., 1994)
   c. Stringency clamping (Roberts & Crothers, 1991)
2. Quantitation of polymerase chain reaction products (Vary, 1992)
3. Nonenzymatic ligation of double-helical DNA (Luebke & Dervan, 1991, 1992)
4. Triplex-mediated inhibition of viral DNA integration (Mouscadet et al., 1994)
5. Site directed mutagenesis (Havre et al, 1993)
6. Detection of mutations in homopurine DNA sequences (Olivas & Maher, 1994)
7. Mapping of genomic DNA
   a. Triple Helix Vector (Moores, 1990)
   b. Artificial endonucleases (Povsic et al., 1992)
   c. Electron microscope mapping (Cherny et al., 1993)
8. Artificial control of gene expression (review Hélène et al., 1992)

Table 1.2: Inhibition of transcription of selected genes via intermolecular triplexes.

Gene	Oligomer (bp)	Inhibition	Conditions	Reference
Human *c-myc*	27	Initiation	in vitro	Cooney et al., 1998
Human *c-myc*	27	Initiation	HeLa cells	Postel et al., 1991
G-free cassette plasmid	15	Elongation	in vitro	Young et al., 1991
Mouse IL2R	28	Initiation	Lymphocytes	Orson et al., 1991
Mouse IL2R	15-acridine	Initiation	HSB2 cells	Grigoriev et al., 1992
Mouse IL2R	15-psoralen	Initiation	HSB3 cells	Grigoriev et al., 1993
E. Coli bla	13	Initiation	in vitro	Duval-Valentin et al., 1992
Human dihydropholate reductase	19	Sp1 binding	in vitro	Gee et al., 1992
Human Ha-ras		Sp1 binding	in vitro	Mayfield et al., 1994
HIV-1	Various	Initiation	in vitro	Ojwang et al., 1994
				Volkmann et al., 1993, 1995
	31, 38	Initiation	MT4 cells	Mc Shan et al., 1992
T7 early promoter	Various	Initiation	in vitro	Ross et al., 1992
Maize *Adh* 1-GUS	Various	Initiation	Protoplasts	Lu & Ferl, 1992

Human platelet-derived growth factor A-chain	24	Initiation	in vitro	Wang et al., 1992
6-16 IRE (interferon inducible)	21	Initiation	in vitro	Roy et al., 1993, 1994
Progesterone responsive gene	38	Initiation	in vivo (transfection)	Ing et al., 1993
HER-2/*neu*	Various	Initiation	in vitro	Ebbinghaus et al., 1993
HER-2/*neu*	Various	Transcription factor binding	in vitro	Noonberg et al., 1994
Erythropoetin	Various	Initiation	in vitro	Imagawa et al., 1994
Human *mdr1*	27	Elongation	CEM-VLB 100 cells	Scaggiante et al., 1994

1.3 Properties of Oligonucleotide Triple Helices

1.3.1 Classification of oligonucleotide triple helices

Oligonucleotide based triple helices can be formed from a variety of strand combinations. Fig. 1.3 shows the two main groups which are classified according to the composition of the third strand. They are called either the pyrimidine or the purine motifs. The sequences constituting the WC core duplex are connected by solid lines (H-bonds) while the diamonds represent the HG- or RHG-hydrogen bonding of the third strand. The solid and dotted lines represent a pyrimidine strand and a purine strand respectively.

Fig. 1.3.1 shows class 1 triplexes formed from a stoichiometric ratio of three independent strands (Pilch *et al.*, 1990a; Plum *et al.*, 1990). A class 2 triple helix forms from two molecules and three combinations are possible depending on the position of the looping sequence(s). Class 2a is a WC hairpin with an independent third strand (Manzini *et al.*, 1990), class 2b is a core duplex with tethered third strand (Xodo *et al.*, 1990) and class 2c is a circular ligand bound to a single strand (Kool, 1991). Class 3 are triplexes formed from a single strand (Sklénar & Feigon, 1990; Häner & Dervan, 1990). Each class was designed for study by specific techniques and their applications will be discussed further.

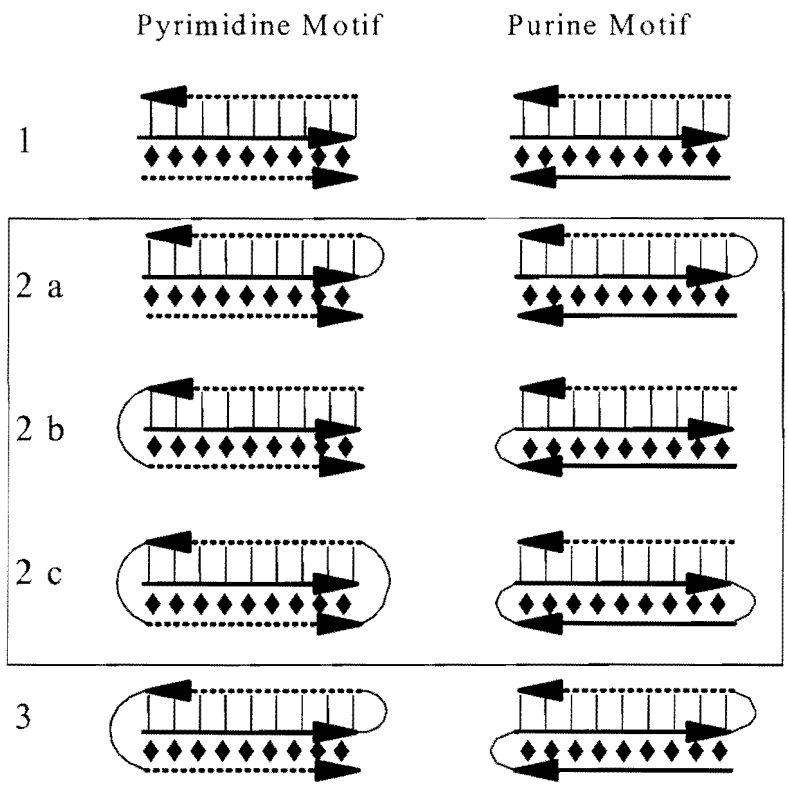

(Adapted from Frank-Kamenetskii & Mirkin, 1995)

Fig. 1.3.1 Classification of oligonucleotide triplexes into two groups, pyrimidine or purine motif, with various classes based on the number of oligonucleotide strands involved. The solid and dotted lines represent a stretch of purine and pyrimidine bases respectively. The vertical, solid lines represent Watson-Crick hydrogen bonding of the underlying duplex. The diamonds represent Hoogsteen or reverse-Hoogsteen hydrogen bonding of the "third strand" in the pyrimidine and purine motifs respectively.

Class 1, triplexes from three independent strands of equal size,

Class 2, triplexes from two independent strands of unequal size:

a, core hairpin plus independent third strand,

b, core duplex plus tethered third strand,

c, circular ligand plus a linear third strand,

Class 3, triplexes from one strand folding back on itself (intramolecular)

1.3.2 Fine structure of triplexes formed from canonical bases

Early X-ray diffraction data and infra red spectroscopy of polynucleotides determined the basic orientation of the third strand as antiparallel to the similar strand of the duplex with *anti*-glycosidic bonds for both the pyrimidine and purine motifs (Morgan & Wells, 1968; Thiele & Gushlbauer, 1969). The cleavage and cross-linking experiments with class 1 oligonucleotides supported these findings (Le Doan et al, 1987; Moser and Dervan, 1987) until Cooney et al. (1988) proposed a parallel orientation for a G, T rich third strand based on DNase footprinting. Cleavage and gel-retardation experiments by the same laboratory later showed the antiparallel orientation of the purine rich strand relative to the purine strand of the duplex (Durland et al., 1991). This was confirmed in the same year by the techniques of affinity cleavage (Beal & Dervan, 1991), photo-footprinting (Frank-Kamenetskii et al., 1991) and NMR (Radhakrishnan et al., 1991). It was concluded that the third strand binds parallel to the duplex purine strand when it is composed of few GpT and TpG steps and antiparallel with many GpT and TpG steps (Sun et al., 1991).

1D and 2D NMR showed directly that an all-pyrimidine strand forms Hoogsteen hydrogen bonding in parallel orientation to the purine strand of the duplex, thus antiparallel to the pyrimidine strand of the duplex (Rajagopal & Feigon, 1989a,b; de los Santos et al., 1989). Computed averages of various helical parameters are shown in Table 3.1. A comparable set of X-ray data is not yet available due to the difficulty of obtaining diffraction-quality crystals (Shafer, 1998).

Table 1.3: Computed averages for various helical parameters. [a]

	Triplexes				Duplexes	
	Pyrimidine		Purine			
	X-ray	NMR	X-ray	NMR	B-DNA	A-DNA
Axial rise (Å)	3.3	3.4	-	3.6	3.4	2.6
Helical twist (°)	31	31	-	30	36	33
Axial displacement (Å)	-2.5	-1.9	-	-1.9	-0.7	-5.3
Glycosidic torsional angle	*anti*	*anti*	-	*anti*	*anti*	*anti*
Sugar pucker	C2'endo	C2'endo	-	C2'endo	C2'endo	C3'endo

[a] (*ex* Frank-Kamenetskii & Mirkin, 1995)

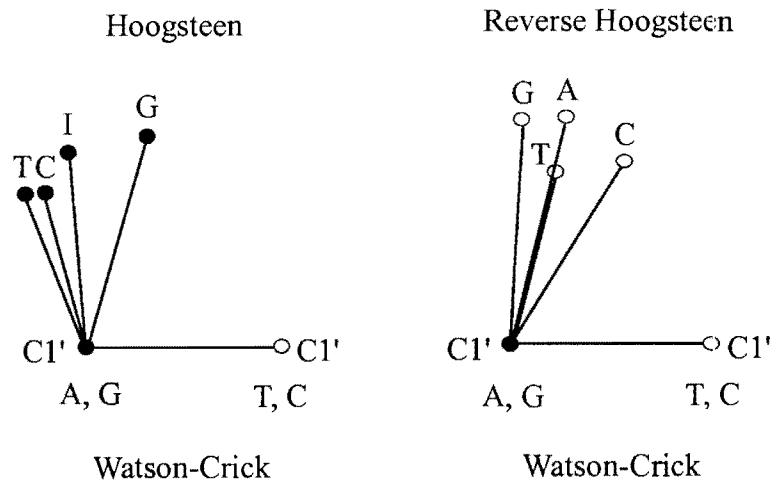

Fig. 1.3.2 The position of the C1' atoms of the three nucleotides shows the isomorphism of "canonical" base triads (adapted from Sun et al. 1991a).

1.3.3 Triplex recognition schemes

The base triads modelled in Fig. 1.1, namely T-AT and C^+-GC in the pyrimidine motif (HG bonding) and T-AT, A-AT & G-GC in the purine motif (RHG bonding) have become known as the "canonical" triads. The canonical triads are described as isomorphous with respect to the orientations of the glycosidic bonds and the positions of the C1′ atom of the three nucleotides. To illustrate this Fig. 1.3.2 shows the position of the C1′ atoms as determined by molecular modelling of 10-mer strands of T-AT and G-GC (Sun et al., 1991a). Although only the pyrimidine motif T-AT and C^+-GC triads are strictly isomorphous, the purine motif triads (Reverse-Hoogsteen base triplets) G-GC, T-AT, and A-AT can be accommodated as seen directly by NMR of specifically designed intramolecular triplexes (Radhakrishnan *et al.*, 1991; Radhakrishnan and Patel, 1993 a, b, 1994 a, b). A protonated A^+-G.C triad can form only at very low pH (Malkov *et al.*, 1993).

Vacuum CD spectra have been used to characterise triplexes containing T and U (Johnson *et al.*, 1991) and the G-G.C triad (Johnson *et al.*, 1992). The G-G.C triad has been further characterised at high resolution by NMR (van Meervelt *et al.*, 1995) and by FTIR (White & Powell, 1995).

1.3.4 Extension of triplex recognition schemes

Unusual triads of natural bases G-TA (Griffin & Dervan, 1989), T-CG and T-GC can be accommodated occasionally within the pyrimidine motif even if they form only a single Hoogsteen hydrogen bond (Beal and Dervan, 1992a). The chemical synthesis of

modified bases for triplex recognition has become a dynamic research field in itself aimed at extending the third-strand binding code (review Soyfer & Potaman, 1996). A classical example is the replacement of cytosine with 5-methyl cytosine which allows formation of the pyrimidine motif closer to neutral pH (Lee et al., 1984, Povsic & Dervan, 1989). The modified triplex is stabilised by about 10°C (Plum et al., 1990). This has been attributed to the replacement of water in the major groove (Xodo et al., 1991).

Another cytosine analogue is 6-oxocytidine which is already protonated (Berressem & Engels, 1995). A guanine analogue 2′deoxyguanosine and a thymine analogue, 7-deaza-2′-deoxyxanthosine, form stable triplexes included in the pyrimidine motif (Milligan et al., 1993). Specific recognition of CG base pairs is demonstrated by 2-deoxynebularine within the purine motif (Stilz & Dervan, 1993).

Other modifications of oligonucleotides can be made with respect to the backbone in an effort to prevent their degradation by intercellular nucleases e.g. incorporating phosphorothioates instead of the usual phosphates. A most interesting development is the introduction of peptide nucleic acids (PNA) which have a peptide backbone and form more stable triple helical complexes than DNA (Egholm et al., 1992).

1.4 Thermodynamics of oligonucleotide triple helix formation

1.4.1 Forces stabilising DNA double and triple helices

The stability of a canonical DNA base pair or base triad depends on the contribution of a) interbase hydrogen bonding, b) stacking interactions between adjacent bases and c) electrostatic interactions between the negatively charged phosphate backbones.

The energy of a hydrogen bond is the difference in energy of an inter-base hydrogen bond and the energy of competing hydrogen bonds between bases and the solvent water. There are 2 hydrogen bonds in an AT base pair and 3 in a GC base pair of double stranded DNA but only 2 hydrogen bonds between a purine HG or RHG base binding as a third DNA strand (Fig. 1.1). The enthalpy of hydrogen bond formation for binding of the third base of a triad should be approximately identical for purines and pyrimidines. This does not take into account the positive charge on a cytosine in the HG of RHG position of a triad which offers an inter- or intrastrand phosphate group interaction. Differences in stability of base triplets must therefore be due to stacking- or electrostatic interactions.

Stacking interactions are made up of a) van der Waals interactions, b) induced dipole interactions (London dispersion forces) and c) hydrophobic interactions. The stability of double stranded DNA can be satisfactorily interpreted in terms of hydrogen bond formation and nearest neighbour interactions from primary structure information (Breslauer et al., 1986; Klump, 1988). The interpretation of the binding

stability of the third strand will have to take into consideration the sequence composition of the duplex but the result cannot be accurately derived from the consideration of hydrogen bonding and stacking interactions alone.

Electrostatic interactions are sequence independent in double stranded DNA as the backbone is uniformly negatively charged. The interaction of monovalent cations with the phosphate backbone is described in terms of the counterion condensation theory (Manning, 1978) or the Poison-Boltzmann Theory (Anderson & Record, 1982). Details of the effects of electrostatic interactions on formation and stabilisation of triplexes are not completely understood. Electrostatic forces involve a) ionic strength dependent, Debye-Hückel screening of the backbone phosphates by counterions and b) site-specific neutralisation of phosphate charges by bound cationic bases such as C^+.

The free energy of binding of a third strand is the sum of the factors described above. It is a challenge to design oligonucleotide systems which allow one to isolate and characterise the contributions of the various forces which affect triplex stability. There are considerably more thermodynamic data available on the denaturation of the double helix than the triple helix because of the stringency of conditions for triplex formation. Assessing a limited data set obtained under varied conditions of pH, ionic strength and strand concentration makes it difficult to make a direct comparison of literature data (review Plum et al., 1995b).

1.4.2 Collection and analysis of thermodynamic data

Thermodynamic parameters can be obtained by differential scanning calorimetry (DSC) and any other technique which records the change in order as a function of temperature under the condition that no intermediate states are populated. DSC measures the excess heat, at constant pressure, (ΔCp) required to induce a transition in a sample compared to the reference buffer. The enthalpy and entropy can be determined by integrating the profiles of ΔCp vs. Temperature (T) and ΔCp/T vs. T respectively. There is no model required to extract the thermodynamic data for the system under study. In contrast a suitable model is required when interpreting UV-melting profiles (A_{260} vs. temperature) by van't Hoff analysis. The process of triplex and duplex melting can be monitored by scanning the absorbance at a particular wavelength (usually 260nm for DNA) over a defined temperature range. On melting the bound strands unstack which is reflected in a characteristic rise in absorbance observed (review Marky & Breslauer, 1987).

A van't Hoff analysis of UV-melting curves is only valid if no intermediate states are significantly populated and this requires careful design of the oligonucleotide system under study. The data derived from UV-melting analysis and DSC do not always match but good comparison can be made between the melting temperatures (T_m) obtained (Manzini et al., 1990; Rougée et al., 1992 & Völker et al., 1993). The technique of UV melting is still used routinely as it requires an order of magnitude less sample concentration than DSC.

1.4.3 Extracting thermodynamic data from a melting profile (Absorbance vs T °C)

Thermodynamic state functions namely enthalpy, entropy and free energy can be extracted from a melting profile according to a published procedure by Marky & Breslauer (1987). The melting temperature (T_m) is defined as the temperature at which 50% of the melting (absorbance change) has occurred. This point is determined according to Fig. 1.4. The melting range (δT) is a reflection of the slope of the curve and contains information about the cooperativity of the transition..

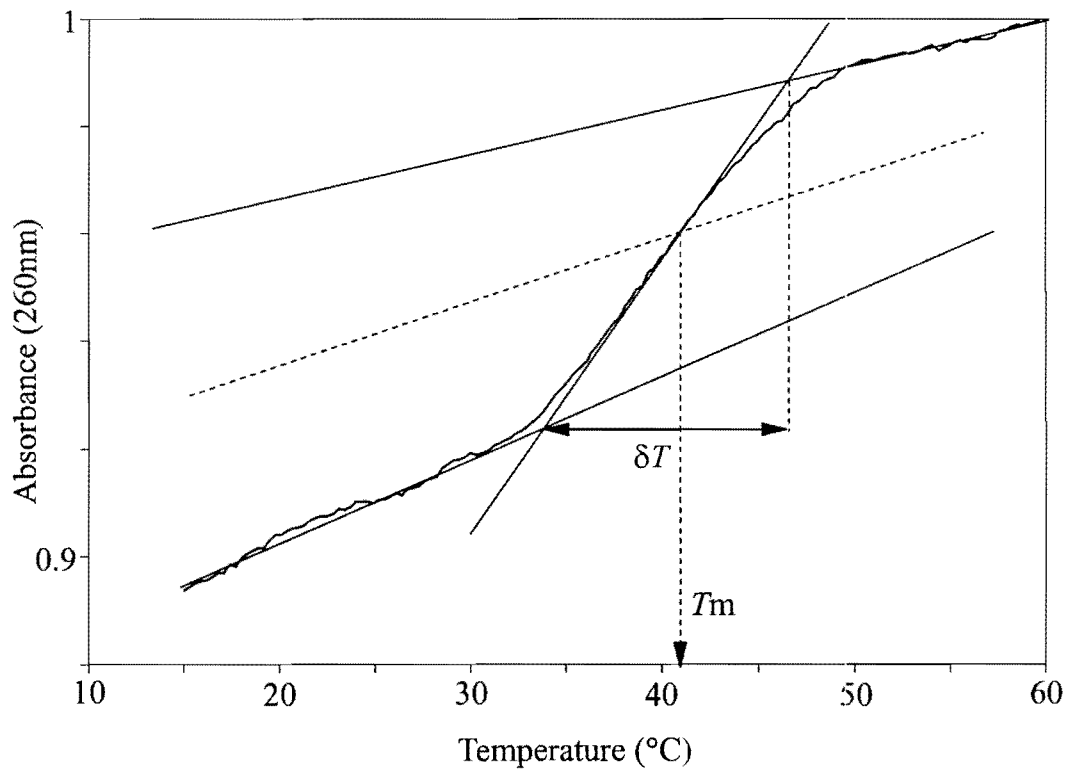

Fig. 1.4 Extracting the T_m from a melting curve (Marky & Breslauer, 1987).

The van't Hoff enthalpy (ΔH_{vH}) can be calculated for a temperature-dependent, co-operative equilibrium reaction according to the equation:

$$\Delta H_{vH} = 2\,(n+1)*R*T_m^2\,(\delta\theta/\delta T)_{Tm} \qquad (1)$$

R is the universal gas constant (2 kcal/mol K), T_m is in Kelvin and $(\delta\theta/\delta T)_{Tm}$ the slope of the curve. The degree of transition $\delta\theta = 1$ for the helix to coil transition as the van't Hoff equation is valid only for true two-state processes. The number of strands is represented by n, which is 2 for the intermolecular reaction of a double helix for example.

Free energy, enthalpy and melting temperature are related through the equation:

$$\Delta G^\circ = -RT \ln K = \Delta H^\circ - T(\Delta S^\circ) \qquad (2)$$

For a bimolecular process where duplex (D) and third strand (M) combine to form triplex (T) the equilibrium association constant (K) is defined as:

$$K = ([T] / ([D] \cdot [M])) \qquad (3)$$

Starting with equal concentrations (C_0) for D and M and if θ is the fraction of the associated species:

$$\mathbf{K = \theta / (C_0 . (1 - \theta)^2)} \qquad \mathbf{(4)}$$

At T_m , θ = 1/2 therefore $K = 2 / C_0$. ΔS_{vH} can then be derived from equation (2) as:

$$\mathbf{\Delta S_{vH} = \Delta H_{vH} / T_m + R.\ln (2 / C_0)} \qquad \mathbf{(5)}$$

For a monomolecular process, such as the triplex-hairpin transition of an intramolecular triplex, the van't Hoff entropy is simply the enthalpy devided by the T_m.

The van't Hoff free energy can then be quoted at a desired temperature calculated according to (6).

$$\mathbf{\Delta G_{vH} = \Delta H_{vH} - T. \Delta S_{vH}} \qquad \mathbf{(6)}$$

1.5 Thermodynamic characterisation of the pyrimidine motif

1.5.1 Triplexes with independent third strands (Classes 1 & 2a)

Table 1.5.1 lists some of the thermodynamic data for independent third strands targeting a WC-duplex or a hairpin i.e. the triplex-duplex equilibrium.. All the data represent the total contribution of hydrogen-bonding and stacking interactions between the duplex and the third strand. The enthalpy and free energy of formation are quoted per base triplet (btp^{-1}). The sequences are ranked according to decreasing length, with the exception of entry 9, and a general trend of increasing stability of the triplex with the length of the third strand is observed. Under similar conditions the class 2a triplexes (entries 4, 5 & 6) are more stable than the class 1 triplexes (7 & 8) (Cheng & Pettitt, 1992a) indicating the role of the conformational entropy in triplex formation.

Table 1.5.1: Thermodynamic data for third-strand dissociation from a duplex or hairpin. *

Entry	Third strand sequence	Length (bp)	Media conditions	T_m (°C)	ΔH/bt (kcal/mol)	$\Delta G_{25°C}$/bt	Reference
1[a]	TTTCCTCCTCTTCTTCTTTTT	22	0.1 M Na^+, pH 6.8	-	-5.0	-	Rougée *et al.* (1992)
2[b]	TTTTTCTCTCTCTCT	15	210 mM Na^+, pH 6.5	30.0	-2.0	-0.09	Plum *et al.* (1990)
3[a]	CCTCTCCTCCCT	12	0.1 M Na^+, pH 5.0	56.0	-4.7	-	Roberts & Crothers (1991)
4[a,c,d]	CTTCCTCCTCT	11	50 mM Na^+, 10mM Mg^{2+}, pH 6.0	62	-5.0	-	Xodo *et al.* (1991)
5[a,c]	CTTCCTCCTCT	11	50 mM Na^+, 10mM Mg^{2+}, pH 5.0	52	-6.6	-	Manzini *et al.* (1990)
6[a,b,c]	CTCTTCTTTC	10	50 mM Na^+, 10mM Mg^{2+}, pH 5.0	-	-5.8	-	Xodo *et al.* (1990)
7[a]	CCCTTTTCCC	10	2 M Na^+, 50mM Mg^{2+}, pH 5.5	29.9	-3.4	-0.75	Pilch *et al.* (1990a)
8[a]	TTTTTTTTTT	10	50 mM Mg^{2+}, pH 7.0	20.6	-2.3	-0.66	Pilch *et al.* (1990a)
9[b]	rA_xU_y (x=5 or 7; y=3-11)		0.1 M Na^+, pH 7.0	- av:	-5.1	-	Ohms & Ackermann (1990)

* Adapted from Soyfer & Potaman (1996)

[a] van't Hoff two-state model from UV or calorimetry, [b] Micro calorimetry, [c] Class 2a, [d] 5-methylated cytosines.

Table 1.5.2: Thermodynamic data for third-strand dissociation from a pyrimidine hairpin targeting a purine strand.

Entry	Third strand sequence	Length (bp)	Media conditions	T_m (°C)	ΔH/bt (kcal/mol)	$\Delta G_{25°C}$ /bt (kcal/mol)	Reference
1[a]	CTCTTCTTTCT	11	50 mM Na^+, 10mM Mg^{2+}, pH 5.0	-	-6.2		Xodo *et al.* (1990)
2[b]	TCCTCCTCC	9	1 M Na^+, pH 5.3	60.0	-15.1	-1.9	Hüsler & Klump (1995b)
3[b]	CTTCTTCTT	9	1 M Na^+, pH 6.0	58.2	-14.3	-8.8	
4[a]	CTTCTCTCC	9	100 mM Li^+, 20mM Mg^{2+}, pH 6.0	41.1	-14.2	-1.6	Mills & Klump (1998)

[a] van't Hoff two-state model from UV, [b] DSC

Table 1.5.3: Predicting the number of protonated Hoogsteen cytosines from thermodynamic data (20 mM Na_2HPO_4, 1 M NaCl; Hüsler & Klump,1995b

Triplex HG strand	pH	ΔH° (kcal/mol)	ΔS (cal/mol K)	T_m (K)	$\partial(1/T_m)/\partial pH$ (10^{-5})	Predicted *n* value	Integer *n*	Number of HG cytosine
TCCTCCTCC	5.3	-135.9 (±5.9)	-399.4 (±24)	333	16.3 (±1)	4.8 (±0.30)	5	6
CTTCTTCTT	6	-128.7 (±5.8)	-679.0(±13)	331.2	9.71(±0.5)	2.7 (±0.14)	3	3

1.5.2 Class 2b triplexes

Table 1.5.2 lists some of the thermodynamic data available for class 2b triplexes. Some more detailed aspects of the pyrimidine motif can be observed. Triplex stability is increased by tethering the third strand compared to the intermolecular approach. This results in a reduction of the conformational entropy due to the proximity of the third strand, which can only move in a small space volume.

Since protonation of cytosine is required for including cytosine in triplex formation the triplex should be stabilised by lowering the pH towards the pKa of free cytosine (c.a. 4.5). The number of cytosines in the third strand have been demonstrated to play a roll in stabilising the triplex as they introduce a local positive charge which helps to neutralise the repulsive effects of the three negatively charged phosphate backbones. Both these properties are elegantly displayed by a three-way junction with triple-helical arms constructed by Paul Hüsler (Fig. 1.5.1). Upon heating of the junction the arms A, B & C dissociate sequentially with the most cytosine rich arm (C) melting last (Hüsler & Klump, 1994, 1995a).

The effect of pH on triplex stability was studied (*cf.* entries 2 & 3 of Table 1.4.2) and compared to a theoretical description derived from the grand partition function with matrix algebra (Hüsler & Klump, 1995b). The experimental and theoretical results are closely matched (Table 1.5.3). The same equation was derived independently by Plum & Breslauer (1995a):

$$n = ((1 / T_m) / \text{pH}).(-\Delta H / R.\ln (10)) \quad (7)$$

where n is the number of protonated cytosines in the triplex; $\partial(1 / T_m)\partial\text{pH}$ is the slope of the linear part of a $1 / T_m$ vs. pH profile; T_m is obtained from UV melting, R is the universal gas constant and ΔH is obtained by DSC. Table 1.5.3 shows the complete data set.

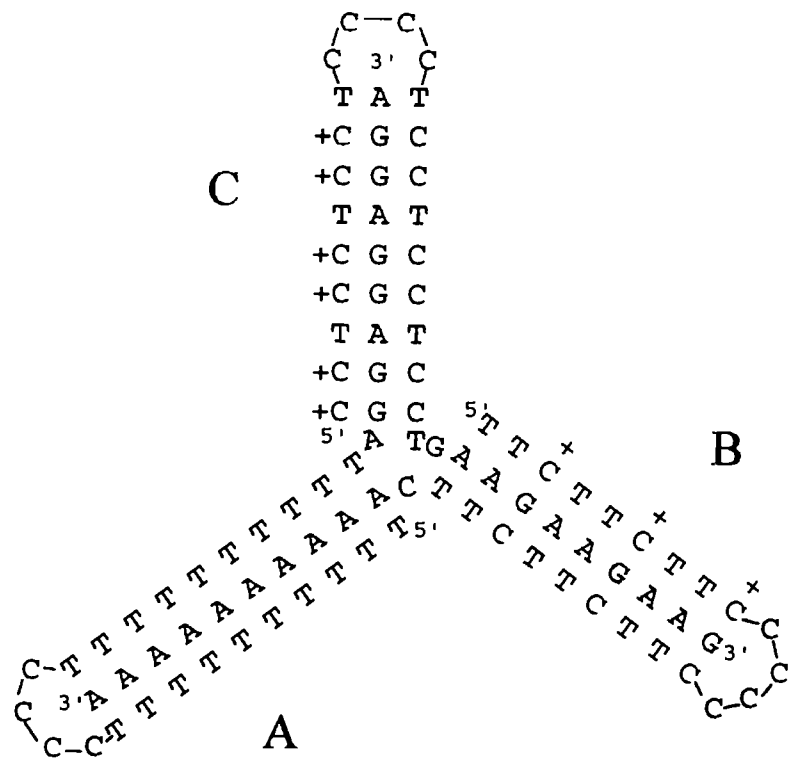

Fig. 1.5.1 A triple helical 3-way-junction of DNA based on the class 2b pyrimidine motif (Hüsler & Klump, 1994).

Table 1.5.4: Thermodynamic data for third-strand dissociation from an intramolecular triplex of pyrimidine motif.

Entry	Third strand sequence	Length (bp)	Media conditions	T_m (°C)	ΔH/bt (kcal/mol)	$\Delta G_{25°C}$ /bt (kcal/mol)	Reference
1[a]	5'-CTCTCTCTTT	10	50 mM Na^+, pH 6.7	41.0	-5.9	-0.15	Völker *et al.* (1993)
1[b]	5'-CTCTCTCTTT	10		41.0	-4.0	-0.19	
2[a]	5'-CTCTCTCTC	9	50 mM Na^+, pH 6.7	32.7	-6.3	-0.16	Mills *et al.* (1996)
3[a]	5'-CTTCTCC	8	1 M Na^+, pH 6.34	30.3	-5.6	-0.10	Plum & Breslauer (1995)
3[b]	5'-CTTCTCC	8		30.3	-2.8	-0.05	

[a] van't Hoff two-state model from UV, [b] DSC

1.5.3 Class 3, intramolecular triplexes

Table 1.5.4 lists some of the thermodynamic data available for the dissociation of the HG strand from a hairpin within an intramolecular triple helix. There are some significant technical and experimental advantages of class 3 triplexes over the other classes with respect to thermodynamic studies (Völker, 1993; Völker et al., 1993).

The orientation of the third strand is fixed with respect to the WC hairpin so mismatches can be introduced into the third strand which under the same conditions might alter the orientation of the third strand in class 1 & 2 triplexes. Being part of a single strand the three "strands" are always in stoichiometric proportions. This reduces the error in concentration determination involved in mixing oligonucleotides. An intramolecular triplex forms in a monomolecular process and consequently the T_m is independent of oligonucleotide concentration allowing straight forward comparison between class 3 triplexes. "Intramolecular structures are thermally more stable than intermolecular structures because of the apparent high local concentration of the strands and the reduced conformational space" (Völker, 1993).

Under certain conditions of pH and counterion concentration the third strand can be observed to melt separately from and before the hairpin to give the data in Table 1.5.4. Fig. 1.5.2 (A) shows the folding pathway of the triplex. The triplex, hairpin and coil conformations can be distinguished with respect to temperature and pH on a phase diagram, a plot of T_m vs pH (Fig. 1.5.2B). This behaviour can also be observed in the other classes but one can observe it over a larger pH and temperature range using intramolecular triplexes because of the inherent stability of the underlying hairpin over a duplex.

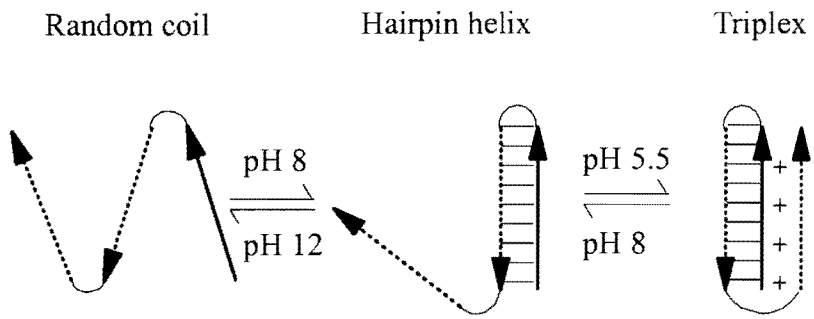

B

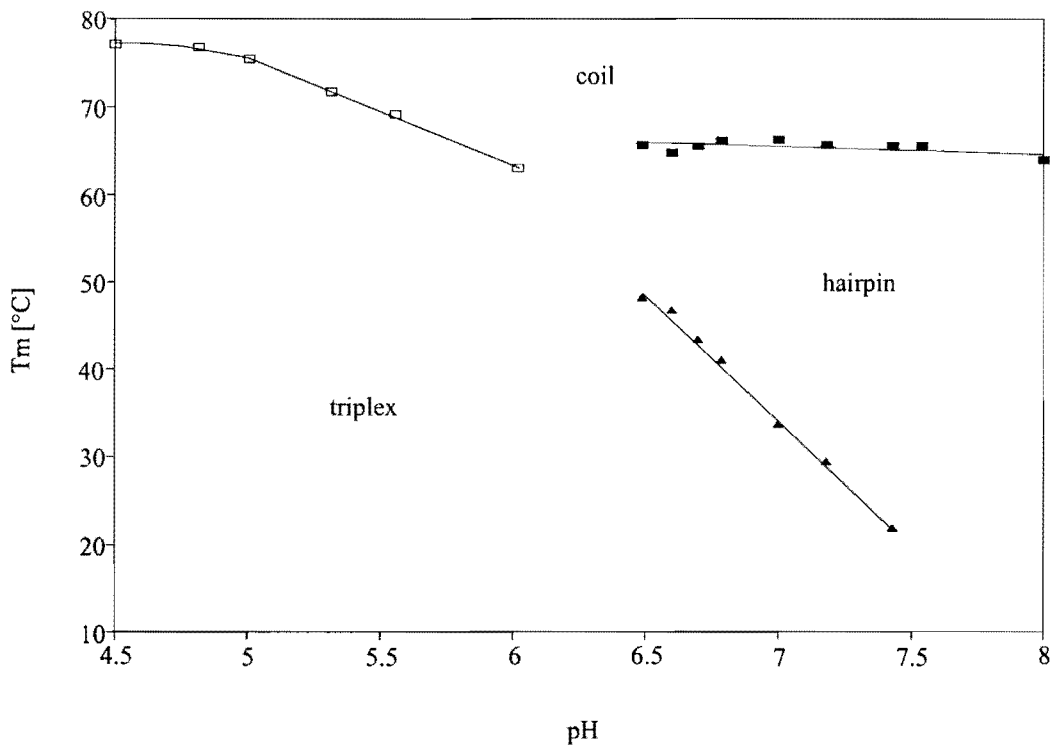

Fig. 1.5.2 A; Schematic of the proposed pH dependent folding pathway of an intramolecular triple helix (adapted from Völker, 1993).

B; Phase diagram (T_m vs. pH) shows the phase boundaries separating the area of stability of the triplex from those of the hairpin and the random coil conformations in 100mM Na^+ (Mills et al., 1996).

1.5.4 The global and local impact of cytosines on third strand stability.

The intramolecular system was adapted to address the importance of electrostatic interactions on the binding energy of the third strand (Völker, 1993; Völker & Klump, 1994). The electrostatic contributions are divided into the sequence-independent repulsive forces between the negatively charged backbones and the sequence-dependent attractive forces provided by the positively charged cytosines. Two families of sequences were characterised with respect to pH and ionic strength to assess the local and global impact of cytosines on the stability of the third strand.

The C^+-GC triad is more stable than the T-AT triad below 400mM Na^+ (pH 6.75) while the converse is true above 400mM Na^+. "At physiological conditions (pH 7.1, 150mM Na^+) thymines and cytosines contribute equally to the stability (global effect) provided that the cytosines are spaced by more than one thymine (local effect)" (Völker, 1993). Consecutive cytosines are unfavourable and it was proposed that perhaps they could be replaced by a neutral base such as inosine which might also remove the pH dependency of triplex formation.

1.5.5 The impact of replacing charged cytosine with "wild-card" inosine.

Inosine is readily accommodated within double stranded DNA (Corfield et al., 1987; Case-Green & Southern, 1994). It was considered an attractive alternative to cytosine in triple-stranded DNA because a) it binds equally well to both GC and AT basepairs and thus could play a role as a "wild card" in TFO's, and b) it does not require protonation making triplex formation pH independent. Characterisation of families of

intramolecular triplexes which systematically incorporate inosine in place of the canonical triads reveals that inosine is a poor substitute (Mills et al., 1996). A single, central I for T replacement in a 9-mer HG strand drops the T_m by about 25°C (*cf.* Shimizu et al., 1994) and about 35°C for two I for T replacements. A single I for C^+ replacement lowers the T_m by about 32° and by 44.5°C for two replacements. This shows that the loss of intramolecular ion pairs between the positively charged cytosines and the backbone phosphates is the more unfavourable influence. Replacing more than two T's or C's with I eliminates the binding of the HG strand at room temperature altogether.

Two consecutive inosines are favoured over two separated by a single base suggesting some stability is gained from stacking interaction. Inosine is of course a large purine base and the deleterious effects observed are also attributed to backbone distortion (Mills et al., 1996). The question then asked was "would inosine be more easily incorporated into an all-purine third strand?"

1.5.6 The impact of mutation in the RHG strand to purine triplex stability.

To answer the question above requires the construction and characterisation of a system in the purine motif similar to the pyrimidine system used above. It turns out that this is not as trivial a task as just rearranging the loop sequences. The design of the sequences presented in this thesis is based on the systematic attempt to construct a system to study the impact of mutation in the reverse Hoogsteen strand by the

intramolecular triplexes which systematically incorporate inosine in place of the canonical triads reveals that inosine is a poor substitute (Mills et al., 1996). A single, central I for T replacement in a 9-mer HG strand drops the T_m by about 25°C (*cf.* Shimizu et al., 1994) and about 35°C for two I for T replacements. A single I for C^+ replacement lowers the T_m by about 32° and by 44.5°C for two replacements. This shows that the loss of intramolecular ion pairs between the positively charged cytosines and the backbone phosphates is the more unfavourable influence. Replacing more than two T's or C's with I eliminates the binding of the HG strand at room temperature altogether.

Two consecutive inosines are favoured over two separated by a single base suggesting some stability is gained from stacking interaction. Inosine is of course a large purine base and the deleterious effects observed are also attributed to backbone distortion (Mills et al., 1996). The question then asked was "would inosine be more easily incorporated into an all-purine third strand?"

1.5.6 The impact of mutation in the RHG strand to purine triplex stability.

To answer the question above requires the construction and characterisation of a system in the purine motif similar to the pyrimidine system used above. It turns out that this is not as trivial a task as just rearranging the loop sequences. The design of the sequences presented in this thesis is based on the systematic attempt to construct a system to study the impact of mutation in the reverse Hoogsteen strand by the

Table 1.6.1: Thermodynamic data for the dissociation of an oligonucleotide triplex helix in the purine motif.

Entry	RHG strand	Length (bp)	Triplex class	Media conditions	T_m (°C)	ΔH/bt (kcal/mol)	ΔG $_{37°C}$ /bt (kcal/mol)	Reference
1[a]	GGAGGAGGAGGAGGGGAGG	20	1	(50 mM Na^+,	79.8			Svinarchuk *et al.* (1995)
2[a]	GGGAGGAGGAGGGGAGG	17	1	10 mM Mg^{2+})	75.9			
3[a]	GGAGGAGGGGAGG	14	1		72.5			
4[a]	GGAGGGGAGG	11	1		72.1			
5[a]	GAGGAGGGAGGA	12	2b	(100 mM Na^+,	71.7		-1.9	Vo *et al.* (1995)
6[a]	GTGGTGGGTGGT	12	2c	10 mM Mg^{2+})	71.0		-1.0 (60°C)	
7[a]	GTGGTGGGTGGT	12	2b		69.3		-1.7	
8[a]	GTGGTGTGTGGT	12	2b		61.0		-1.5	
9[a]	GGGG	3	3	(100 mM Na^+)	64.0			Chen (1991)
10[a]	GGGAAAAGGG	10	1	(10 mM Na^+,	54.0	-15.3	-2.1	Pilch *et al.* (1991)
				50 mM Mg^{2+})		-11.6[b]		Scaria & Schafer (1996)
11[a]	GGTGTGTTG	9	2b	(100 mM Li^+,	42.6	-8.9	-1.1	Mills & Klump (1997)
12[a]	GGAGAGAAG	9	2b	10 mM Mg^{2+})	42.9	-8.4	-1.1	

[a] UV (van't Hoff), [b] Calorimetry. N.B. The thermodynamic data above reflect a triplex-to-monomer transition.

1.6.2 Divalent cation dependency

A universal feature, in contrast to the pyrimidine motif, is the requirement for divalent or multivalent cations to stabilize the purine motif triplex. H-DNA formation was shown to be Mg^{2+} dependent (besides requiring supercoiling) and switching from Mg^{2+} to Zn^{2+} affected the equilibrium between isoforms (Kohwi & Kohwi-Shigematsu, 1988, 1993). Comparison of A-AT and T-AT triads by chemical footprinting showed the trend: A-AT (Mn^{2+})>T-AT (Mn^{2+})>T-AT (Mg^{2+})>A-AT (Mg^{2+}) (Washbrooke & Fox, 1994).

1.6.3 The effect of monovalent cations

The purine motif is also affected by monovalent cations which can inhibit triplex formation with K^+ and Rb^+ being most effective followed by NH^{4+}, while Na^+ and Li^+ have little or no adverse effect (Cheng & van Dyke, 1993). The effect of monovalent cations on a class 1 purine triplex is shown in Fig. 1.6. The fraction of triplex formed is deduced from electrophoretic mobility shift titrations and related to the ionic radius of the cations in the buffer (Olivas & Maher, 1995). Cations with ionic radii between 1-1.5Å have the most inhibitory effects (K^+, NH_4^+, Rb^+).

1.6.4 G-rich strands form competing structures

The amount of data available on the purine motif is even less than the pyrimidine motif and certainly more controversial. Interpretation of the data is made more difficult as G-rich oligonucleotides can form alternative structures. Competing

equilibria are possible in the presence of Na^+ as G-rich strands favour quadruplex formation over triplex formation via G-quartets (Scaria *et al.*, 1992). Stretches of GA repeats within a sequence are also susceptible to self-structure formation (Noonberg *et al.*, 1995). The effect of sequence composition on purine triplex stability has thus become a topic of recent interest (Cheng & Van Dyke, 1994; de Bizemont et al., 1996; Faucon et al., 1996).

```
A              3' GGGTGGGTGGTGGG
                  ♦♦♦♦♦♦♦♦♦♦♦♦♦
B        5' GATCCGCGTGGGAGGGAGGAGGGCCCGGATC
              |||||||||||||||||||||||||||||
C        3' CTAGGCGCACCCTCCCTCCTCCCGGGCCTAG
```

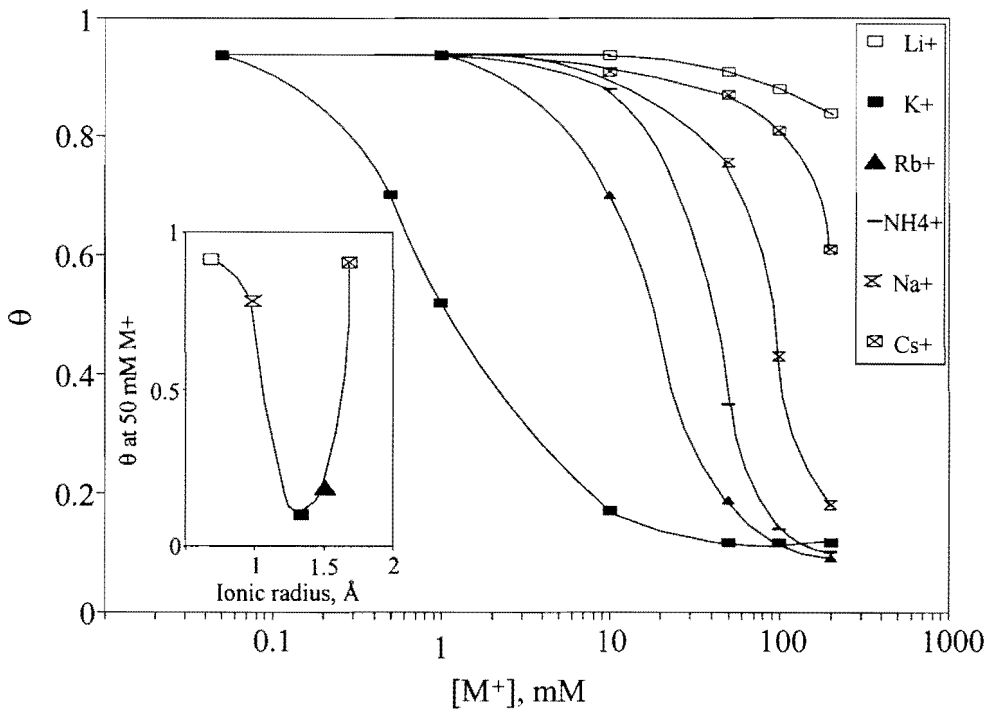

Fig. 1.6 Effects of different M^+ on duplex/triplex equilibria. Triplex inhibition curves for 1μM A, binding target duplex B + C (adapted from Olivas & Maher, 1995).

1.6.5 Investigating an intramolecular purine triplex

An ideal triplex which allows study of the stability of the RHG third strand and the core WC helix should have biphasic melting behaviour as well as the experimental advantages of the intramolecular system. In an attempt to create such a system the intramolecular construct of Mills et al.(1996) was altered from the pyrimidine to the purine motif (Table 1.6.2).

Table 1.6.2: Oligonucleotide sequences designed to form intramolecular triplexes.

Entry	Structure	Motif	Reference
1	5′ GAGAGAGAAA C C T CTCTCTCTTT C T T CTCTCTCTTT	Pyrimidine	Völker *et al.* (1993)
2	5′ GAGAGAGAG C C T C CTCTCTCTC T T T CTCTCTCTC	Pyrimidine	Mills *et al.* (1996)
3	5′ CTCTCTCTC T T C T GAGAGAGAG C T C GTGTGTGTG	Purine	Potential triplex

After initial inspection of the potential intramolecular purine triplex (entry 3, Table 1.6.2) the partial sequences were made asymmetrical to avoid the formation of a competing hairpin between "strands" 1 and 3 where strand 3 is the RHG strand containing G and A. Two arrangements of "strands" are possible depending on the position of the pyrimidine stretch i.e. 5' purine-purine-pyrimidine or 5' pyrimidine-purine-purine. Table 1.6.3 shows results of preliminary UV-melting experiments comparing the T_m's and magnesium dependencies of the various sequences

1.6.5 Investigating an intramolecular purine triplex

An ideal triplex which allows study of the stability of the RHG third strand and the core WC helix should have biphasic melting behaviour as well as the experimental advantages of the intramolecular system. In an attempt to create such a system the intramolecular construct of Mills et al.(1996) was altered from the pyrimidine to the purine motif (Table 1.6.2).

Table 1.6.2: Oligonucleotide sequences designed to form intramolecular triplexes.

Entry	Structure	Motif	Reference
1	5′ GAGAGAGAAA CTCTCTCTTT CTCTCTCTTT	Pyrimidine	Völker *et al.* (1993)
2	5′ GAGAGAGAG CTCTCTCTC CTCTCTCTC	Pyrimidine	Mills *et al.* (1996)
3	5′ CTCTCTCTC GAGAGAGAG GTGTGTGTG	Purine	Potential triplex

After initial inspection of the potential intramolecular purine triplex (entry 3, Table 1.6.2) the partial sequences were made asymmetrical to avoid the formation of a competing hairpin between "strands" 1 and 3 where strand 3 is the RHG strand containing G and A. Two arrangements of "strands" are possible depending on the position of the pyrimidine stretch i.e. 5' purine-purine-pyrimidine or 5' pyrimidine-purine-purine. Table 1.6.3 shows results of preliminary UV-melting experiments comparing the T_m's and magnesium dependencies of the various sequences

Table 1.6.3: Melting temperatures (T_m) for a set of oligonucleotides designed to form potential intramolecular purine-motif triple helices or their underlying hairpin duplexes.

Entry	Structure	T_m [a] (°C)	$dT_m/d\log[Mg^{2+}]$ (1-10 mM) (°C)
1	5′ GAAGAGAGG T T T T GAAGAGAGG C C T C C GTTCTCTCC	71	5.2 ± 0.6
2	5′ CCTCTCTTC C C C C GGAGAGAAG T T C T T GGAGAGAAG	71	4.2 ± 0.2
3	5′ GTTGTGTGG T T T T GAAGAGAGG C C T C C CTTCTCTCC	67	4.6 ± 0.1
4	5′ GAGAGAGAG C C CTCTCTCTC T T	67	7.3 ± 0.5
5	5′ CCTCTCTTC C C GGAGAGAAG T T	66	6.9 ± 0.2
6	5′ CCTCTCTTC C C C C GGAGAGAAG T T C T T GGTGTGTTG	65	5.2 ± 0.6

[a] Buffer conditions: 10 mM sodium cacodylate, 2 mM magnesium chloride, pH 7.0

1.7 Pyrimidine and purine motifs can compete for the same duplex

The canonical triads show a GC base pair can be targeted by a C^+ in the pyrimidine motif and a G in the purine motif and an AT base pair can bind T in both the pyrimidine and purine motifs. It will be shown below that an oligonucleotide system can be constructed to demonstrate that a Hoogsteen strand can compete with a Reverse Hoogsteen strand for the same duplex within the same molecule. The complex is a sensitive system to detect the influence of A and T in the RHG strand. Changes in stability of the RHG strand are reflected in the change in T_m of the triplex and the shift of the triple point in a phase diagram of T_m vs pH. The choice of counterions are 100mM Li^+ to avoid G-Quartet formation (Radhakrishnan et al., 1991; Olivas & Maher, 1995) and 20mM Mg^{2+} to induce the purine motif.

2.1 Oligonucleotide Synthesis and Purification

All oligonucleotides in Table 2.1 were synthesised by conventional phosphoramidate chemistry (Narang, 1987) with one of the following automatic synthesisers:

1) An Autogen 6500 (Miligen, Burlington Mass.) with double-coupling to drive the reaction to completion. Purification was by trityl selection on a Pharmacia Mono Q anion-exchange column (Völker *et al.*, 1993) with an elution gradient of 50 mM to 3 M LiCl in 10mM NaOH. The tritylated oligonucleotides were precipitated overnight in 6 volumes of ethanol/acetone (1:3) and centrifuged at 15k for 30 min. Resuspension in concentrated ammonia followed with desiccation under vacuum. The dimethoxytrityl group was removed with a 1 hr treatment in 80% acetic acid. The DNA was precipitated in butanol and resuspended in double-distilled water. The oligonucleotides appeared as single bands on 20%, denaturing electrophoresis gels. Oligonucleotide concentrations were determined specrophotometrically at 260nm and 80°C with molar extinction coefficients calculated using C, 7400; T, 8700, G, 11500; A, 15400 and I, 12000 M^{-1} cm^{-1} (Cantor & Schimmel, 1980).

2) A Beckman 1000M DNA synthesiser with purification by reverse phase HPLC on an acetonitrile gradient.

3) Ordered from Eurogentec (Belgium) and used without further purification.

Table 2.1: Oligodeoxynucleotide sequences and computed extinction coefficients[1].

Name	Sequence 5'to 3'	ε (x10^5 M^{-1} cm^{-1})
9Y	CCTCTCTTC	0.72
$9Y_{INV}$	CTTCTCTCC	0.72
9R	GAAGAGAGG	1.19
22Y	CCTCTCTTC CCTT CTTCTCTCC	1.76
22RT	GAAGAGAGG CCTT GGTGTGTTG	2.44
$22RA_5$	GAAGAGAGG CCTT GGTG**A**GTTG	2.50
$22RA_{3,5}$	GAAGAGAGG CCTT GG**A**G**A**GTTG	2.57
$22RA_{7,8}$	GAAGAGAGG CCTT GGTGTG**AA**G	2.57
$22RA_{3,5,7}$	GAAGAGAGG CCTT GG**A**G**A**G**A**TG	2.64
22R	GAAGAGAGG CCTT GG**A**G**A**G**AA**G	2.70
$22RI_5$	GAAGAGAGG CCTT GGTG**I**GTTG	2.47
$22RI_{3,5}$	GAAGAGAGG CCTT GG**I**G**I**GTTG	2.51
$22RC_5$	GAAGAGAGG CCTT GGTG**C**GTTG	2.42

[1] Extinction computed using C, 7400; T, 8700; G, 11500; A 15400; I, 12200 $M^{-1}cm^{-1}$

(Cantor & Schimmel, 1980)

2.2 UV-Melting

Thermal denaturation monitored by UV Absorbance was carried out in the following spectrophotometers:

1) A Pye-Unicam SP1800 with a custom made heating block interfaced to an IBM PC through an Oasis A/D converter. Absorbance values were recorded at 260nm every 0.3°C at a heating rate of 1°C/min. Samples containing 2.5μM of each oligonucleotide were heated to 80°C for 3 minutes, allowed to cool to room temperature over 60 minutes to avoid alternative folding intermediates and then stored at 4°C for 60 minutes prior to scanning. The melting temperatures (T_m) were extracted from the digitised data by a computer-based curve-fitting procedure (Hüsler & Klump, 1994) and processed with the Quattro-Pro software package.

2) A Uvikon 940 spectrophotometer interfaced to an IBM-AT personal computer. The temperature of the cell holder was maintained by a Haake P2 waterbath and controlled by a Haake PG 20 thermoprogrammer to give a cooling and heating cycle at a rate of 0.2 °C /min. Absorbencies were recorded at 260nm and subtracted from a baseline recorded at 500nm. Thermodynamic data were extracted according to Marky & Breslauer (1987).

Solutions were mixed from (X2) buffer of 200mM LiAc, 40mM $MgAc_2$, 40mM NaCacodylate or 40mM Tris-Acetate with aliquots of 1M $MgCl_2$ or $MgAc_2$. The pH was adjusted with acetic acid and measured with a Swiss-Lab 300 pH meter.

2.3 Gel retardation experiments (PAGE)

Electrophoresis was performed with a 0.5 mm thick, 15% poly-acrylamide/bisacrylamide (19:1) non-denaturing gel in a 50 mM 2-(N-morpholino)ethane-sulfonic acid (MES) buffer (pH 6) containing 10 mM $MgCl_2$. Oligonucleotides were ^{32}P labelled with T_4 kinase. Samples were denatured and allowed to cool slowly to anneal with incubation overnight at 4°C in 50 mM MES (pH 6), 10 mM $MgCl_2$, 10% sucrose, 1 μM carrier oligo dT_{26}, 1 μM cold oligo, then loaded and run at 120 V for 6 hours.

Results & Discussion

3.1 Proposed folding pathway of the "Limulus structure"

Figure 3.1A represents the proposed folding pathway for the formation of the two alternative complexes assembled from 22Y/22RT called the "Limulus structure" as it resembles a Horseshoe crab with a large carapace and a thin tail. Depending on the environmental conditions it is made up of either the control purine triplex (9Y/22RT) with a single strand extension or pyrimidine triplex (22Y/9R) Figs. 3.1B & 3.1C respectively. Sequence 22Y is a palindrome of pyrimidine bases separated by a mismatching loop sequence (CCTT). Sequence 22RT has two unequal halves. On the 5′ end it has G & A as the first 9 bases to complement the one half of 22Y. The two 5′-half sequences combine to form a core Watson-Crick duplex in the presence of monovalent cations. The 5′ purine tract is followed by the loop (CCTT) sequence and another purine tract of G's & T's.

On addition of divalent cations e.g. Mg^{2+} the 3′ G/T extension of 22RT folds back and binds onto the core duplex to form a purine motif triple helix. Alternatively, on lowering the pH, protonation of cytosine occurs which will now allow the formation of the pyrimidine motif triplex as the pyrimidine tail displaces the Hoogsteen purine strand to bind on the core duplex. The pyrimidine motif can also form at low pH in the absence of Mg^{2+}. The pyrimidine motif is in principle Mg^{2+} independent and pH dependent, while the purine motif is Mg^{2+} dependent and pH independent.

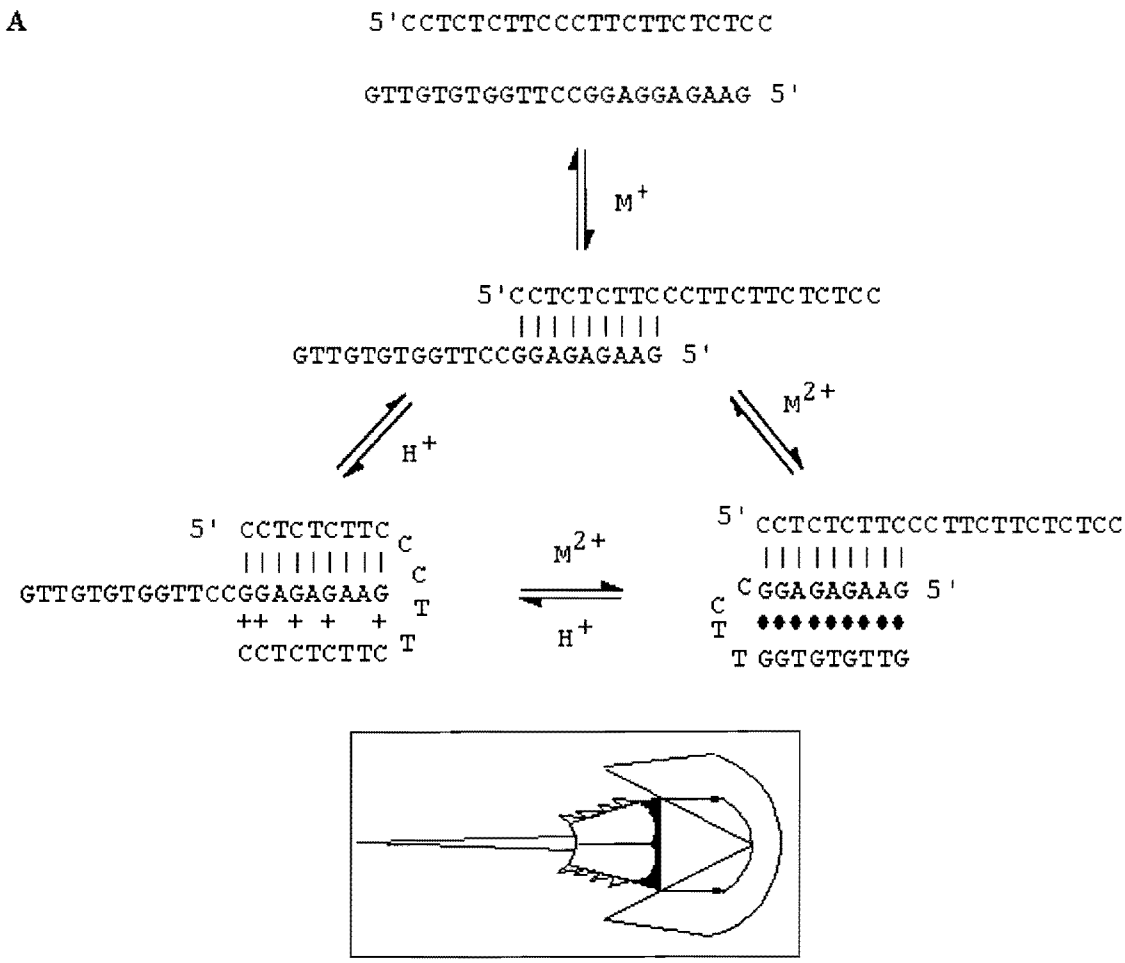

Figure 3.1A Proposed folding pathway for the "Limulus" structure (22Y/22RT).

The inset is a cartoon of a *Limulus*, Horseshoe crab.

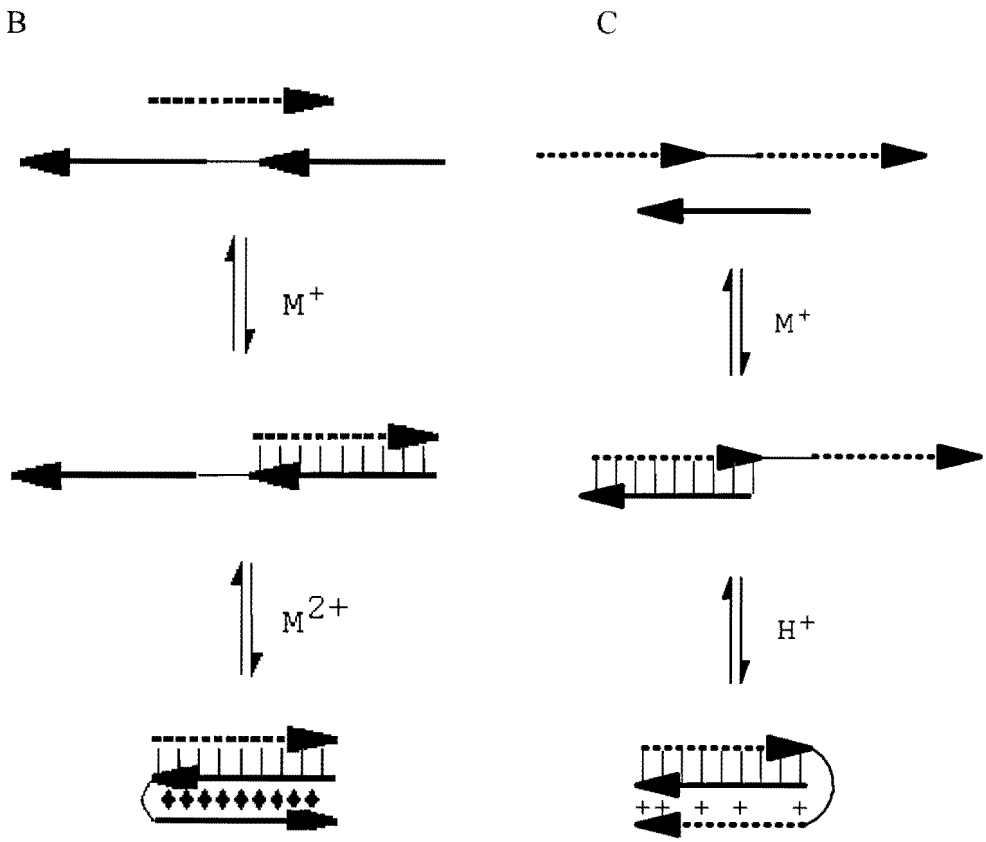

Figure 3.1B Proposed folding pathway for the control purine triplex (9Y/22RT) & C, control pyrimidine triplex (22Y/9R).

3.2 Characteristic melting profiles

Figure 3.2A shows characteristic UV cooling and melting profiles (Absorbance *vs* temperature) at pH 6.0 for 22Y/22RT recorded at two wavelengths. The cooling and melting profiles are superimposable indicating a two-state transition and rapid formation kinetics (the temperature change is 0.2°/min). All complexes studied gave reproducible curves of this nature and were analysed as two state transitions to obtain the T_m (Marky & Breslauer, 1987). The reporter wavelength of 295nm shows a hypochromism associated with the change in environment of protonated cytosine (Fresco & Klemperer, 1959). The T_m's at 260nm and 295nm are identical indicating that this is the melting of the pyrimidine triplex to coil. The pyrimidine motif melts monophasically in the presence of 20mM Mg^{2+} at pH 6.0. It will be shown later to melt biphasically in the absence of Mg^{2+} at pH 7.0 (Fig. 3.8.2).

Figure 3.2B shows a comparison of the first derivative of melting curves of the duplex (9Y/9R), control purine triplex (9Y/22RT) and "Limulus structure" 22Y/22RT at pH 7.0. All curves are monophasic at 260nm and lack the hypochromic shift at 295nm of the pyrimidine motif. The profile for 22Y/22RT (triangle) is similar to the profile characteristic for the control purine triplex (9Y/22RT, open square) and their maxima (T_{max}'s) coincide. The complex 22Y/22RT, which is most probably in the purine motif conformation, has a higher T_m than the duplex (filled square). It is noticeable that very little increase in hyperchromicity is observed for the melting of the purine motif over the core duplex. The control purine triplex is compared to the duplex in more detail later on (Ch. 3.7).

A

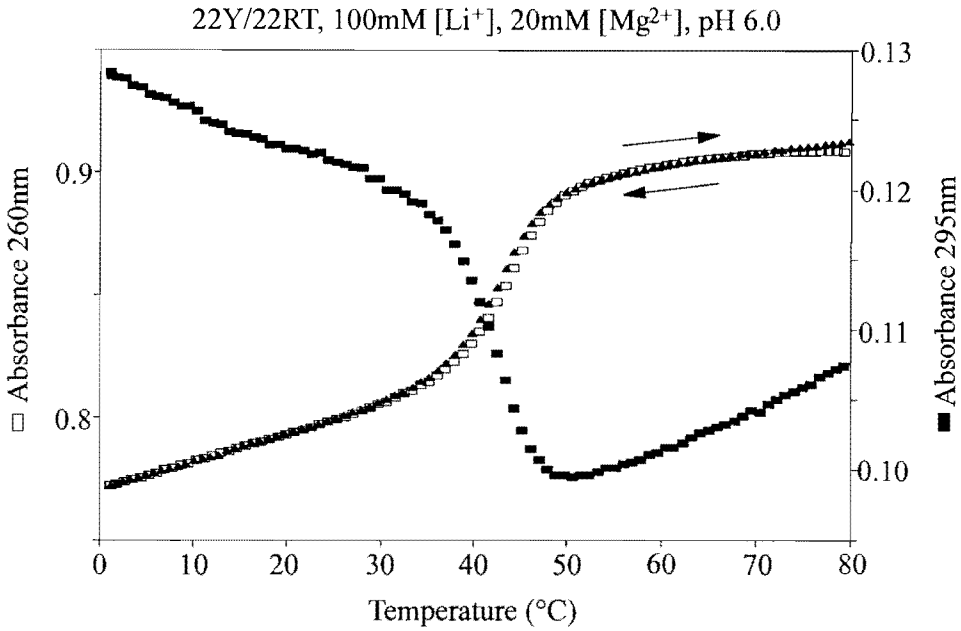

B

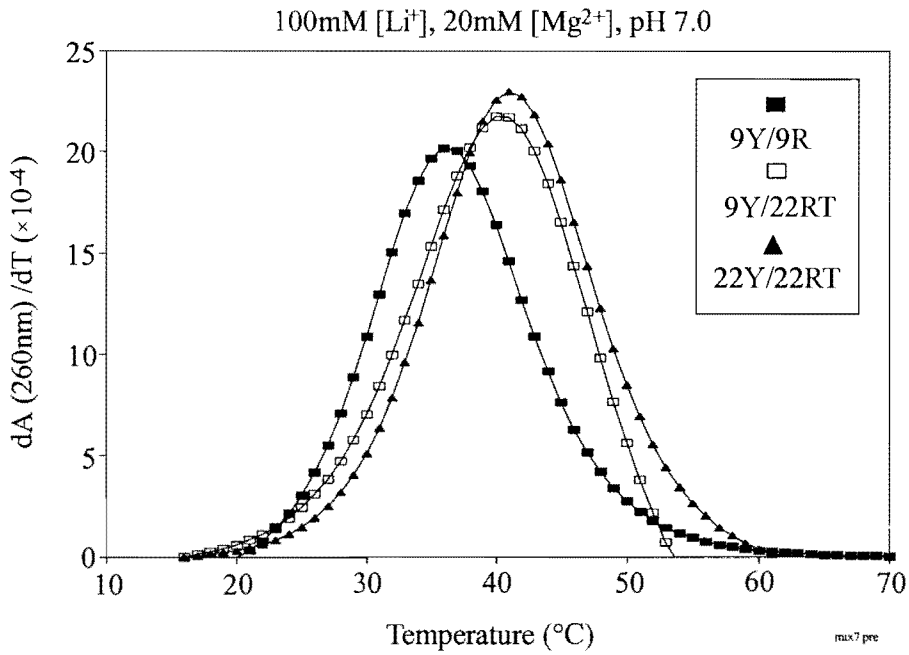

Figure 3.2A, Characteristic cooling and melting profile of 22Y/22RT at pH 6.0;

B, Comparing derivative plots of profiles for the duplex 9Y/9R and triplexes 9Y/22RT and 22Y/22RT at pH 7.0 (100mM [Li^+], 20mM [Mg^{2+}]).

3.3 Thermodynamic data

3.3.1 The purine tailed "Limulus" is preferred at pH 6

Thermodynamic data extracted from melting profiles recorded at 260nm are presented in Table 3.3.1. At pH 6.0 the T_m of the control purine triplex is only about 3°C higher than the T_m of the core duplex which melts at 35°C in 100mM Li^+ & 20mM Mg^{2+}. Both transitions yield a van't Hoff enthalpy (ΔH_{vH}) of -62 kcal/mol as the melting profiles have similar shape (Svinarchuk, 1995). The control pyrimidine triplex has a T_m 6°C higher than the core duplex and the corresponding transition enthalpy ΔH_{vH} is twice the amount of the duplex (-128 kcal/mol). This is characteristic for a class 2b pyrimidine triplex to coil transition (Hüsler & Klump, 1994). The stable conformation at pH 6 of 22Y/22RT is the pyrimidine motif with the purine extension. It is slightly more stable than the control triplex 22Y/9R. This may be due to the fact that the "open" end of the triplex is not blunt and some stacking interaction may be gained from interaction within the free 3′ extension.

3.3.2 "Limulus" adopts the purine motif at pH 7

At pH 7.0 the duplex and combination of 22Y/9R melt concurrently (within 1°C) supporting the conclusion that a duplex is formed with a dangling 3′ extension. The control purine triplex and the complex 22Y/22RT also show almost identical T_m's of 39.8°C and 39.4°C respectively indicating the Limulus is in the purine mode. The enthalpy values are not as informative as the T_m and an average transition enthalpy of 64 (±11) kcal/mol is observed for the complexes at pH 7 resembling the duplex-coil

transition. These enthalpy values, derived from the shape of the melting profile, should be compared to values derived from the concentration dependence of the T_m. This experiment (future work) will confirm the bimolecular nature of the melting transition and will lead to a calorimetric study at higher DNA concentration. The competition between the two alternative triplex motifs can best be demonstrated with the help of a phase diagram of T_m *vs* pH.

Table 3.3.1: Comparing thermodynamic data for the "Limulus" structure (22Y/22RT) with the duplex (9Y/9R) and control triplexes (9Y/22RT & 9R/22Y) in 20mM [Li^+], 20mM [Mg^{2+}] with 2.5μM strands.

pH	Complex	T_m[b] (°C)	$-\Delta H_{vH}$[b] (kcal/mol)	$-\Delta S_{vH}$ (cal/mol K)	$-\Delta G°_{25°C, vH}$ (kcal/mol)
6.0[a]	9Y/9R	35.2	62	174	10.2
	9Y/22RT	38.3	62	172	10.8
	22Y/9R	41.4	128	380	14.8
	22Y/22RT	43.2	113	330	14.6
7.0[a]	9Y/9R	36.3	73	209	10.8
	9Y/22RT	39.8	56	152	10.8
	22Y/9R	37.4	49	131	10.1
	22Y/22RT	39.4	76	216	11.6

[a] Buffer: 20mM Na Cacodylate, 100mM LiAc, 20mM $MgAc_2$

[b] Uncertainty in T_m of 1°C and 10% for other thermodynamic parameters.

3.4 Competing triplex motifs are revealed in a phasediagram of T_m vs pH

Figure 3.4 depicts phase diagrams (T_m *vs* pH) for the various constructs in 100mM Li^+ & 20mM Mg^{2+} between pH 5.0 and 8.0. "These diagrams will have two useful applications. From the diagram the conformational state of the poly/oligonucleotides in the system at any arbitrary set of external conditions (pH/T) can be taken simply by inspection. From the behaviour of the phase boundaries, the physical effects responsible for the phase transitions can be assessed" (Klump, 1987).

Figure 3.4A shows the behaviour the core duplex whose formation is considered pH independent. The phase boundary is indicated by a solid line which represents a distribution of 50% duplex to 50% single strands. The duplex has a slight stability maximum around pH 7.5 and shows a gentle decrease in stability as the pH is lowered to 5.0. Figure 3.4B, in addition, shows how much the pH must be lowered before the pyrimidine 3′ extension of 22Y folds on to the core duplex to form a pH dependent triple helix. The dotted line is a hypothetical boundary which is not easily determined from the monophasic melting profile. There is a linear increase in T_m with decreasing pH between pH 6.2 and 5.0 for the triplex-coil transition showing the influence of the protonated cytosines. Figure 3.4C describes the pH dependency of the control purine triplex which melts consistently at a slightly higher temperature than the duplex within this pH range. The phase boundary follows a corresponding trend to that of the duplex highlighting the similarity of the duplex-coil and triplex-coil transitions.

Figure 3.4D shows clearly the various phases (areas of stability) of the alternative structures formed from 22Y/22RT. The purine "Limulus" is stable above pH 6.1 and below 40°C. Below pH 6.1 the pyrimidine "Limulus" is stable and gains stability in a

linear fashion with decrease in pH towards the pKa of free cytosine. The phase triple-point is well defined suggesting that at about 40°C and pH 6.1 all three conformations coexist with no degree of freedom for the external conditions.

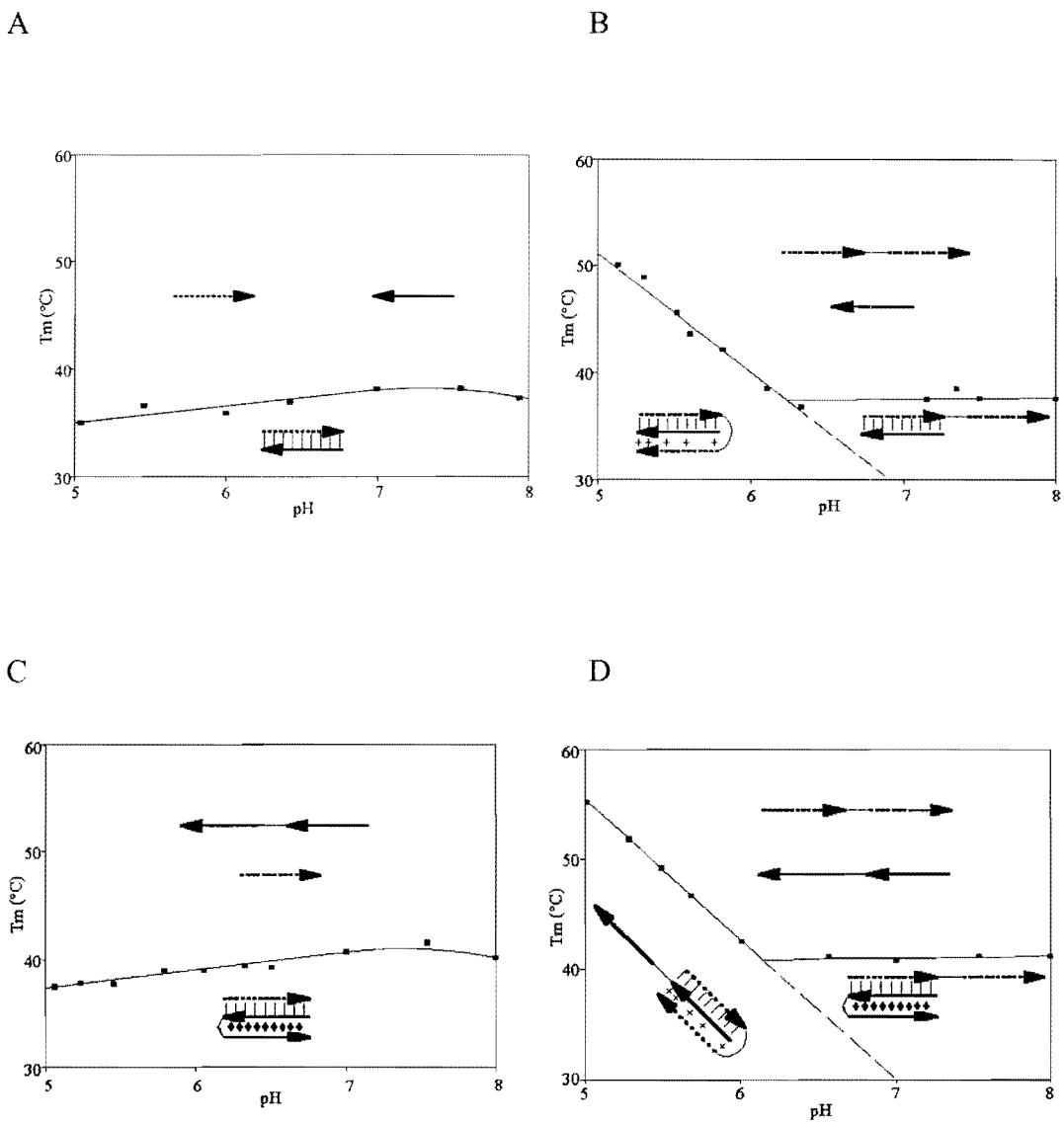

Figure 3.4 Phase-diagrams (T_m vs pH) in 100mM [Li^+], 20mM [Mg^{2+}]: A, duplex (9Y/9R); B, pyrimidine triplex (9Y/22RT); C, purine triplex (22Y/9R) and D, alternative "Limulus motifs" (22Y/22RT).

3.5 The effect of counterions

3.5.1 Magnesium ion concentration dependency

The effect of increasing the magnesium ion concentration from 20mM to 50mM on the phase boundaries is shown in Figure 3.5.1. All the phase boundaries and consequently the triple point shift. Both the purine triplex-coil and pyrimidine triplex-coil boundaries are parallel shifted to higher triplex stability resulting in an increased T_m by 4.3°C and 2.7°C respectively. The triple point is effectively shifted down to pH 6.0 from 6.1 and up by 4.3°C. The pyrimidine motif is relatively less stabilised because there are already formal charges present on the cytosines of the RHG strand. The phase diagram demonstrates that the "Limulus" is a flexible and sensitive system for detecting the effects of Mg^{2+} on the two triplex motifs.

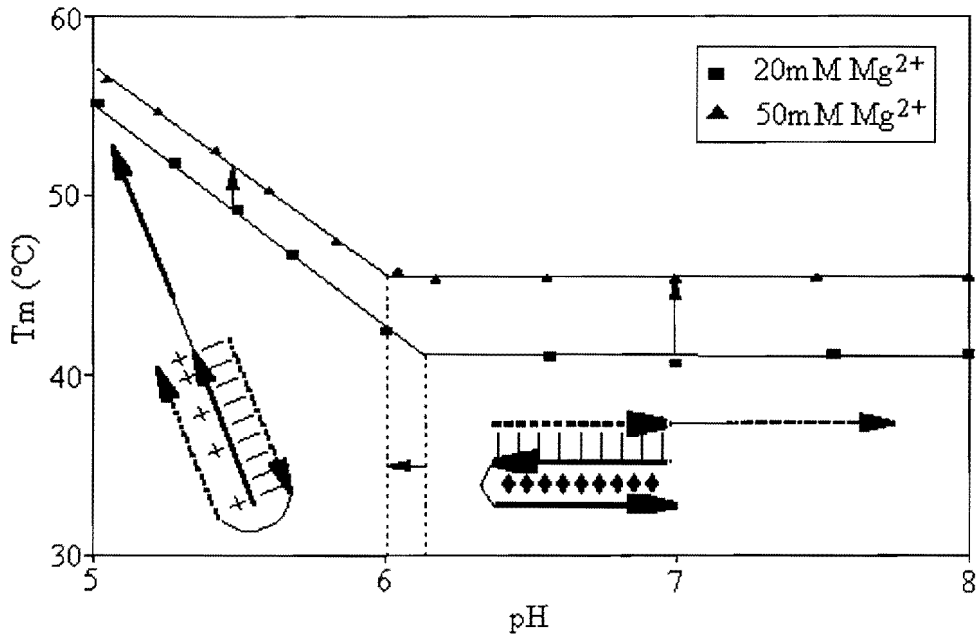

Figure 3.5.1 Effect on the T_m of 22Y/22RT on increasing the [Mg^{2+}].

To test for the influence of monovalent ions a phase diagram was created by increasing the concentration of Na^+ ions.

3.5.2 Sodium ion concentration dependency

Figure 3.5.2 shows the effect on the phase diagram of adding 1M Na^+ to the solution of 100mM Li^+ and 20mM Mg^{2+}. The phase boundaries remain unchanged and there is no extra stabilisation observed. However it cannot be concluded that Na^+ has no effect on either triplex motif's stability. The divalent cation concentration of 20mM is considered sufficiently high already to mask the effects of additional monovalent ions (Noonberg et al., 1995). To observe the impact of monovalent cations the phase diagram should be recalibrated to explore the lower limit of magnesium ion concentration suitable to form a stable purine triplex. A comparison in the presence of K^+ ions (approaching physiological conditions) would then be possible. The phase diagrams suggest the purine triplex will be favoured over the pyrimidine triplex under physiological conditions.

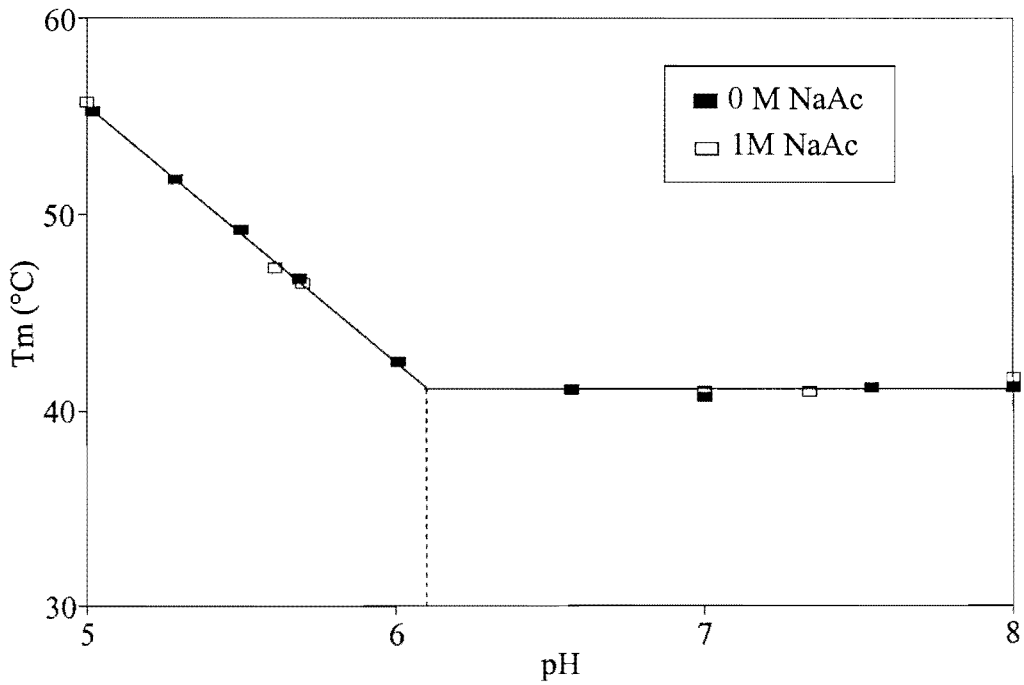

Figure 3.5.2 Phase diagram of T_m vs pH for 22Y/22RT in 100mM [Li^+], 20mM [Mg^{2+}] with and without 1M [Na^+].

3.6 The effect of sequence composition

3.6.1 The effect of exchanging T for A in the RHG strand of the control purine triplex

Tables 3.6.1 and 3.6.2 list the thermodynamic data for the purine triplexes ranked according to T_m for a series in which adenine systematically replaces thymine in the RHG strand. The changes in T_m are relatively small and so an effort was made to amplify the differences by increasing the magnesium ion concentration. The data is presented in Figure 3.6.1 as a 3D plot of T_m vs number of thymines replaced vs magnesium concentration for the control purine triplex.

Three trends are apparent from the 3D plot: (i) there is an expected general increase in T_m with the increase in $[Mg^{2+}]$ as the counterions dampen the repulsive effects of the three negatively charged, intertwined, sugar-phosphate backbones. (ii) As thymines are systematically replaced by adenines there is an increase in T_m of about 4°C (at 20mM Mg^{2+}) until 50% of the RHG strand consists of adenine (i.e. 2 thymines have been replaced), then there is a decrease in T_m until all 4 thymines are replaced by adenine. (iii) The $[Mg^{2+}]$ dependency of the triplex stability follows a similar trend with the 50% substituted triplex ($9Y/22RA_{3,5}$) showing an increase of about 2°C in slope over the all-thymine triplex (9Y/22RT).

The observed trends are in line with the following explanation. With the substitution of adenine for thymine there are favourable stacking interactions introduced to the RHG strand as a purine base is larger than a pyrimidine base and stacks more

effectively on a purine. Once the two thymines which are closest to the loop have been replaced it appears that an optimum stacking unit has been formed and further substitution only serves to reverse the trend, perhaps by distorting the duplex. These results are in line with the findings of Vo *et al.* (1995) who reported that the A-A.T triad is preferable to the T-A.T triad in a system in which a palindromic, 12-mer hairpin containing G and A is 2.4 °C more stable than the corresponding hairpin with G and T in the RHG strand (100mM Na^+, 10mM Mg^{2+}). This unusual trend is revisited later on (Ch.3.7).

Table 3.6.1: Thermodynamic data for the purine motif ($22RT_x/9Y$) with mutations in the Reverse Hoogsteen Strand (RHG) ranked according to melting temperature (T_m)[a].

Ligand	Reverse Hoogsteen Strand 5′to 3′	T_m[b] (°C)	$-\Delta H_{vH}$[b] (kcal/mol)	$-\Delta S_{vH}$ (cal/mol K)	$-\Delta G°_{25°CvH}$ (kcal/mol)
$22RA_{3,5}$	GG**A**G**A**GTTG	46.9	73	201	13.1
$22RA_5$	GGTG**A**GTTG	45.3	82	230	13.3
$22RA_{3,5,7}$	GG**A**G**A**G**A**TG	44.2	88	250	13.4
22RA	GG**A**G**A**G**AA**G	42.9	76	213	12.4
22RT	GGTGTGTTG	42.6	80	226	12.6
9R	GAAGAGAGG	35.9	86	251	11.1

[a] Buffer: 100mM LiAc, 20mM $MgAc_2$, 20mM Tris-Ac (pH 7.0) with 2.5μM strands.

[b] Uncertainties are estimated at 0.5°C for T_m and 10% for thermodynamic parameters.

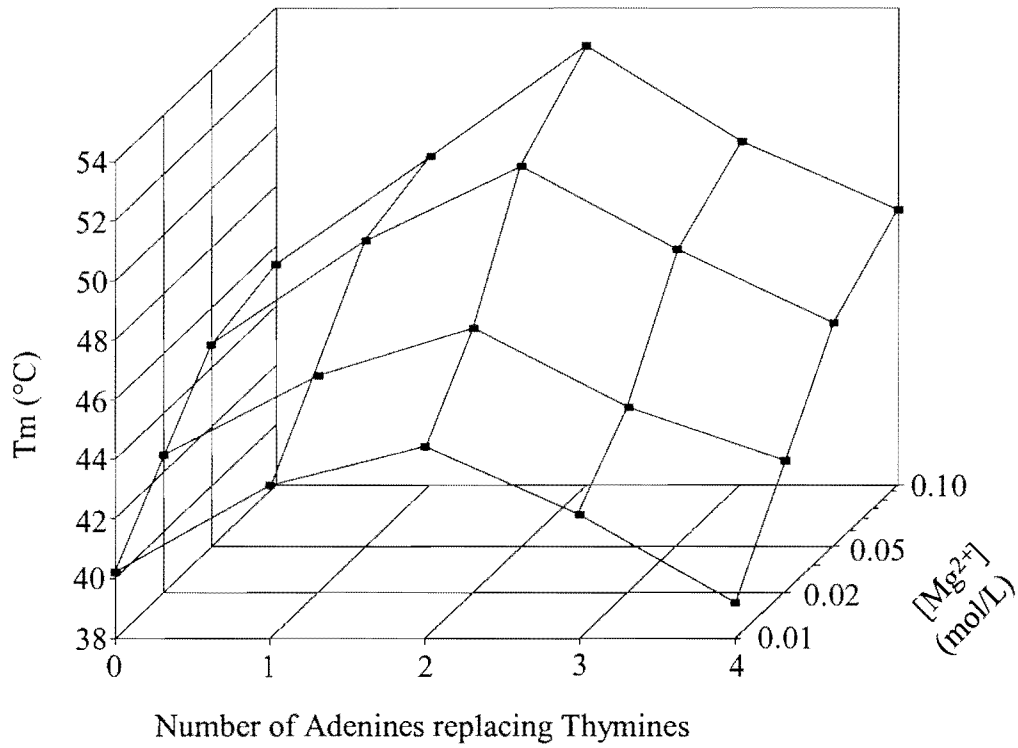

Figure 3.6.1 A 3D plot of Number of Adenines replacing Thymines in the Reverse Hoogsteen Strand of purine triplex $22RT_x/9Y$ *vs* T_m *vs* $[Mg^{2+}]$ (log scale).

Radhakrishnan et al. (1993) concluded from their chemical shift data (NMR) that replacing an A-AT triple with a T-AT triple has no effect on the conformation of the neighbouring triples. They did, however, observe a preference for T-AT over A-AT triples in shifting the equilibrium towards the triplex. They found this to be consistant with the affinity cleavage studies of Beal & Dervan (1991). This created the impression that the T-AT triad is always favoured over the A-AT triad. Figure 1.6.1 above shows that the exchange of T for A initially improves the stability until a maximum stability is reached at 50% exchange. Increasing the number of A`s beyond this ratio seem to decrease the stability again. There are no general rules extractable from either the thermodynamic or the structural data as to what extend a homopurine sequence, in a reverse-Hoogsteen strand, is binding more strongly than a mixed or homopyrimidine sequence.

3.6.2 The effect of exchanging T for A in the RHG strand of the "Limulus structures"

Figure 3.6.2 is a compilation of 5 phase diagrams superimposed in a 3D plot of T_m vs pH vs number of T's replaced for A's. The magnesium concentration is fixed at 20mM with 100mM [Li^+]. Several important trends can be observed:

(i) The slopes (pH dependencies) of all triplex-coil transitions remain unaffected by the T to A mutation. (ii) There is a concomitant increase in T_m of the purine triplex until 3 T's are replaced by A. (iii) Replacing all 4 T's with A results in a subsequent drop in T_m. (iv) At pH 5.0 all pyrimidine motifs melt at the same T_m irrespective of the number of mutations. (v) The triple-points of the phase diagrams are shifted to lower pH and higher temperature following the increased stability of the purine "Limulus". The trend appears to be linear and is presented in a plot of number of T's replaced by A *vs* the intercepting pH of the phase diagrams (Figure 3.6.3).

The Limulus system is sensitive enough to detect the effect of systematically replacing T with A in the RHG strand. The A-AT triad is preferred over the T-AT triad within the purine motif. The system has an advantage over the two control triplexes as the replacement of 3 T's in the RHG strand sustains the trend observed. An explanation for this observation lies in the possibility that the 3′ single-strand extension gives some stabilising stacking interaction which is lacking in the blunt-ended control triplex as already seen for the pyrimidine motif.

A disadvantage of the "Limulus structure" over the control triplex becomes obvious on replacing all T with A. The sequence becomes a palindrome and either half of 22RA could act as the reverse Hoogsteen strand and competing structures arise. Whether this results in a decrease in stability has to be shown. To investigate the competing structure further a reference system is presented (Ch.3.7.5) with the triplex formed by 22RA and the inverse sequence of the pyrimidine strand ($9Y_{INV}$).

Table 3.6.2: Thermodynamic data for the purine motif ($22RT_x/22Y$) with mutations in the Reverse-Hoogsteen strand ranked according to melting temperature (T_m)[a].

Ligand	Reverse Hoogsteen Strand 5′ to 3′	T_m[b] (°C)	$-\Delta H_{vH}$[b] (kcal/mol)	$-\Delta S_{vH}$ (cal/mol K)	$-\Delta G_{vH}$ (kcal/mol)	$-dT_m/dpH$[c] (°C/pH unit)
$22RA_{3,5,7}$	GG**A**G**A**G**A**TG	45.5	52	136	11.5	11.6
$22RA_{3,5}$	GG**A**G**A**GTTG	43.5	78	219	12.7	10.6
22RA	GG**A**G**A**G**AA**G	42.2	79	223	12.4	13.2
$22RA_5$	GGTG**A**GTTG	41.3	63	173	11.4	11.8
22RT	GGTGTGTTG	40.0	66	184	11.3	12.9
9R	GAAGAGAGG	36.3	83	241	11.1	11.1
av:						12 (±1)

[a] 100mM LiAc, 20mM $MgAc_2$, 20mM Tris-Ac (pH 7.0) with 2.5μM strands.

[b] Uncertainties are estimated at 0.5°C for T_m and 10% for thermodynamic parameters.

[c] Slope represents the pH dependency of the pyrimidine motif.

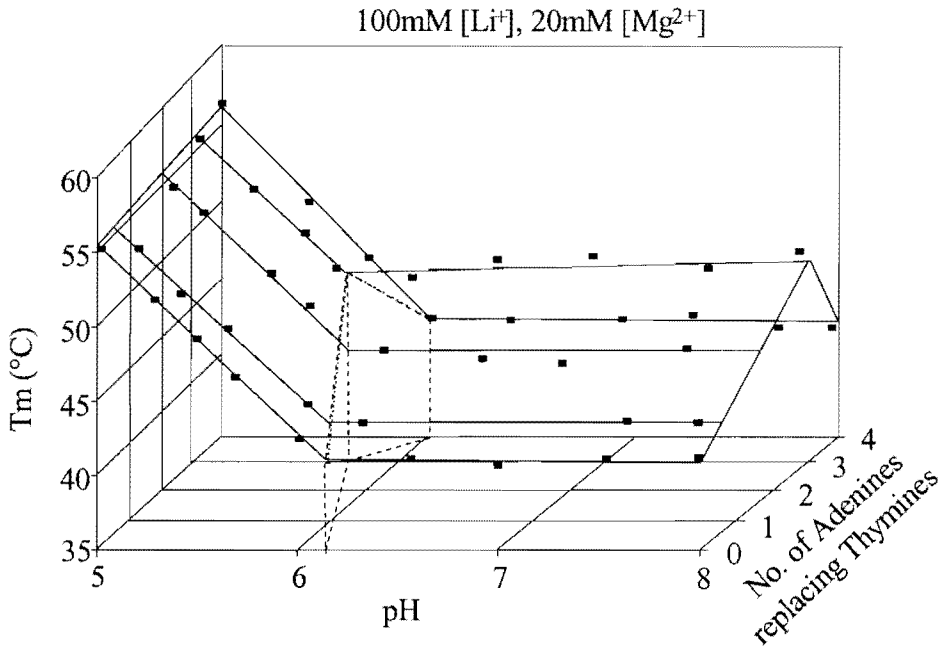

Figure 3.6.2 A 3D plot showing T_m vs pH vs number of Thymines replaced by Adenines in the Reverse Hoogsteen Strand of the "Limulus" structure (22Y/22RT).

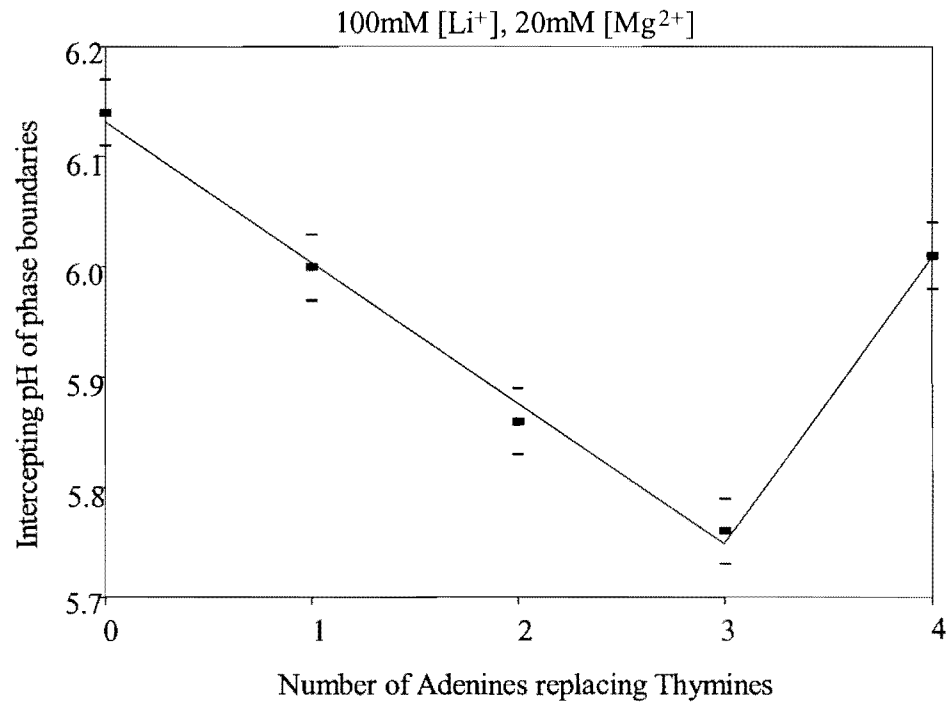

Figure 3.6.3 Equilibrium pH between pyrimidine "Limulus" and purine "Limulus" conformations with respect to sequence composition.

3.6.3 Comparing the experimental value obtained for the number of protonated cytosines in the pyrimidine "Limulus" and control triplex (22Y/9R).

The pH dependency of the pyrimidine "Limulus" and the control triplex (22Y/22R) fall within the average determined from all the triplex derivatives listed in the final column of Table 3.6.2. The dT_m/dpH values can be incorporated into equation 7 (page 30) along with the van't Hoff enthalpy values, quoted at pH 6, in Table 3.3 to arrive at the number of protonated cytosines in the Hoogsteen strand. The number of cytosines in the Hoogsteen strand sequence is 5 and the predicted integer value of protonated cytosines within the triplex is 4. A possible explanation for the discrepancy is that the two consecutive cytosines on the 3′ end share a proton between them. The terminal cytosine cannot make a strong a bond as it has only one neighbouring base with which to stack. This explanation is in line with the observation of Hüsler & Klump (1995b) *cf.* Table 1.5.3.

3.7 Characterisation of the control purine triplex

3.7.1 Characterisation of the reference purine triplex (9Y/22RT) with respect to the underlying duplex (9Y/9R)

Figure 3.7.1 depicts the proposed folding pathway for the triple helix based on the purine motif constructed by linking the Crick and Hoogsteen strands via a CCTT loop to target the Watson (pyrimidine) strand. In the presence of monovalent cations only the complementary Watson and Crick sequences bind to form a core 9-mer duplex with a 3′ 13-mer, single-strand extension of the Crick strand. On addition of divalent cations the 3′ tail folds on to the duplex to form a stable Reverse-Hoogsteen (RHG) triple helix consisting of G-GC and T-AT triads.

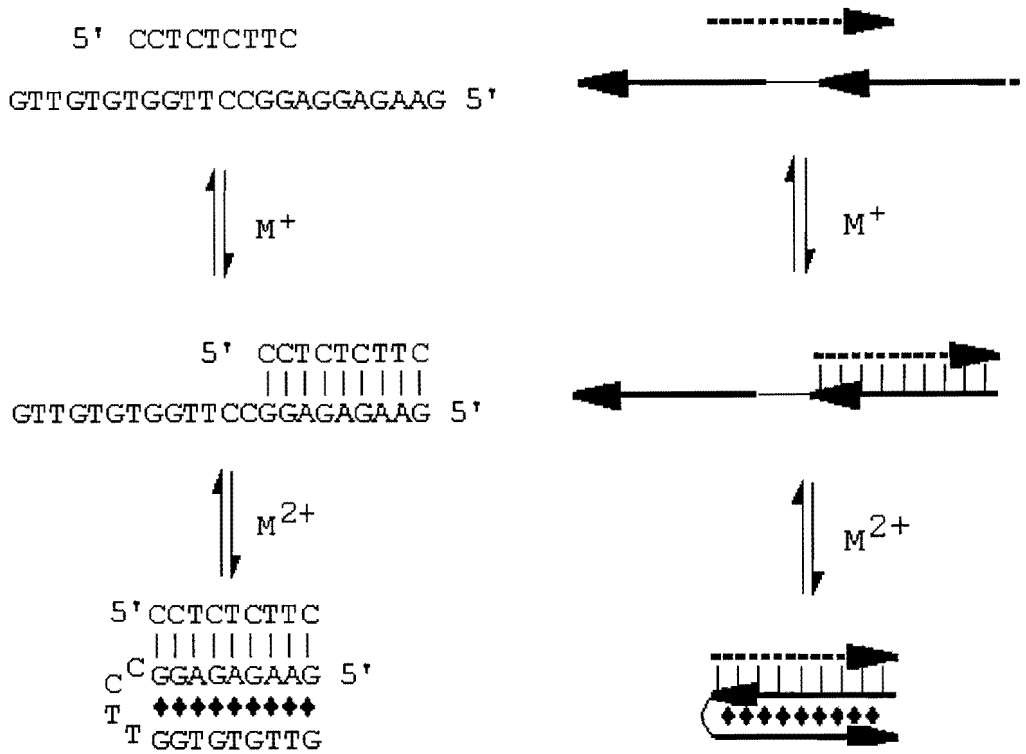

Figure 3.7.1 Proposed folding pathway for the formation of a triple helix based on the purine motif.

The melting profile of the purine triplex is shown in comparison to the core duplex and the purine-rich single strand (22RT) in Figure 3.7.2. The insert shows normalised-Absorbance at 260nm *vs.* Temperature profiles for the 22mer strand alone (22RT, filled triangles), which shows some gradual increase in absorbance but no co-operative melting curve. This is different from the duplex (filled squares) and purine triplex (open squares) which both present sigmoidal melting profiles. Both order/disorder transitions are monophasic and this is consistent with the related system of Vo *et al.* (1995) and both the intermolecular and intramolecular systems of Svinarchuck *et al.* (1995) and Chen (1991) respectively.

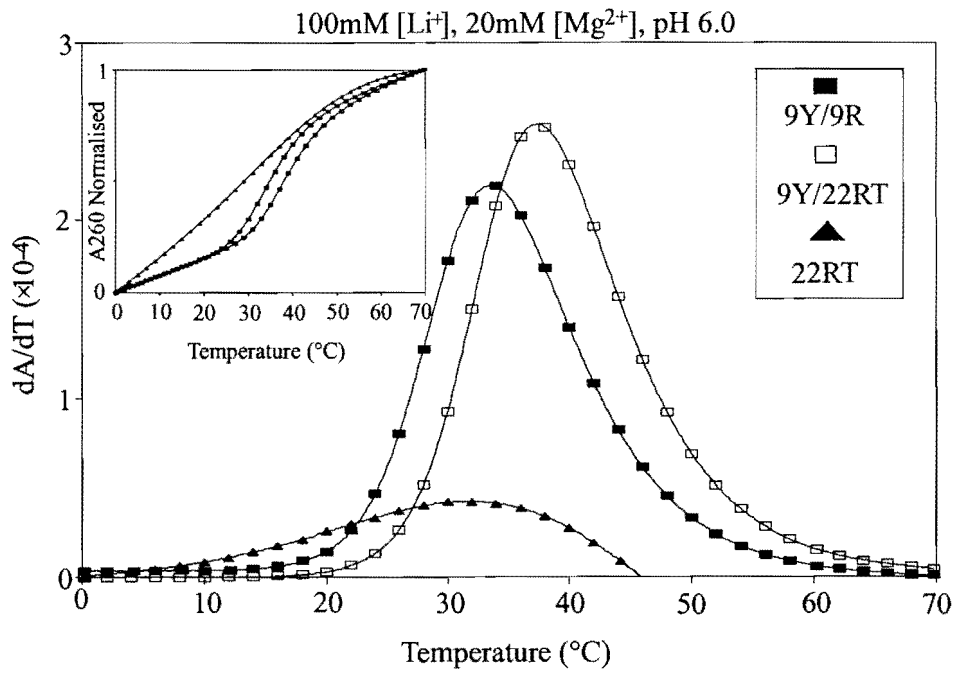

Figure 3.7.2. First derivative melting profiles with an insert of normalised melting curves of duplex (9Y/9R, filled squares), purine triplex (9Y/22RT, open squares) and single strand (22RT, filled triangles).

The profiles produced on cooling are identical to those produced on heating (0.2 °C/min) for the duplex and all triplexes indicating rapid and reversible complex formation. The derivative melting profiles of the ordered structures are very similar in shape. This can be seen as an indication that the triplex melts directly to the coil state and that there is no sizeable population of duplex-with-a-tail intermediate at pH 6.0.

Figure 3.7.3 shows the magnesium concentration dependency of the stability of purine triplex 9Y/22RT compared to the duplex (9Y/9R). In the absence of Mg^{2+} the melting temperatures are identical. This is an indication that the triplex does not form and the stable conformation is the double helix with the 3′ extension. Both duplex and triplex are not significantly stabilised beyond 50mM Mg^{2+}. The $d(T_m)/d(\log [Mg^{2+}])$ between 10mM and 50mM Mg^{2+} is 2.2 (±0.1) °C and 6.5 (±0.7) °C for duplex and triplex respectively in 100mM [Li^+] at pH 7.0.

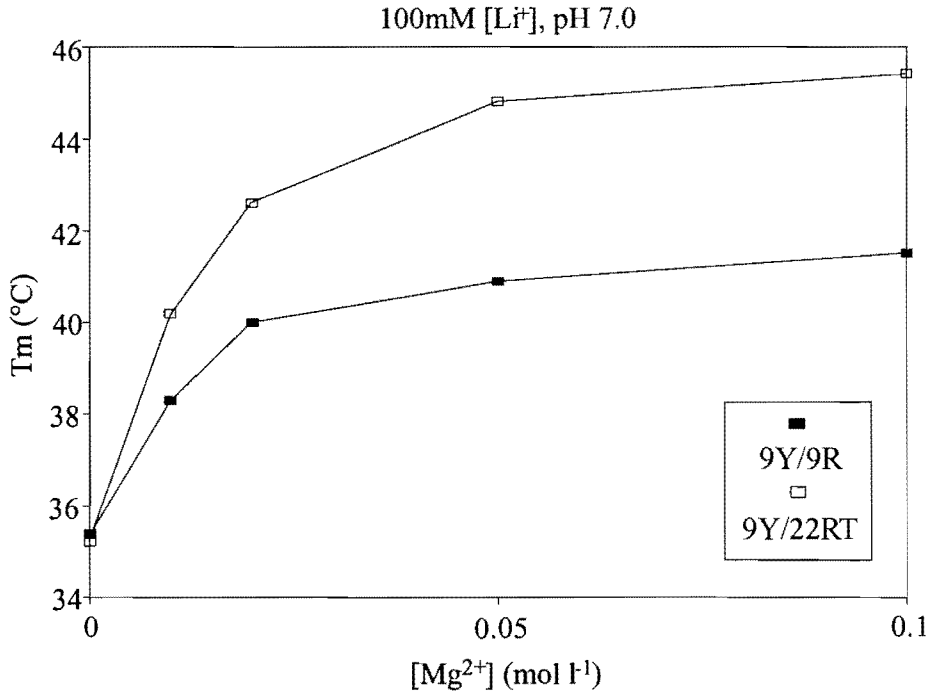

Figure 3.7.3 Melting temperatures (T_m) of duplex-coil and purine triplex-coil transitions *vs.* magnesium concentration in 100mM LiAc, 20mM Tris-Ac (pH 7.0).

Another way to distinguish the control triplex from the duplex is by non-denaturing gel electrophoresis. Figure 3.7.4 shows a scan of a gel carried out at 4°C in which the concentration of labelled target strand (9Y*) is kept constant and either the same strand or complementary strand (9R) or the 22mer ligand (22RT) are added in increasing concentration. Three distinct bands are observed and labelled as single strand (ss), duplex (ds) and triplex (ts) exhibiting increasing retardation related to the size of the complex.

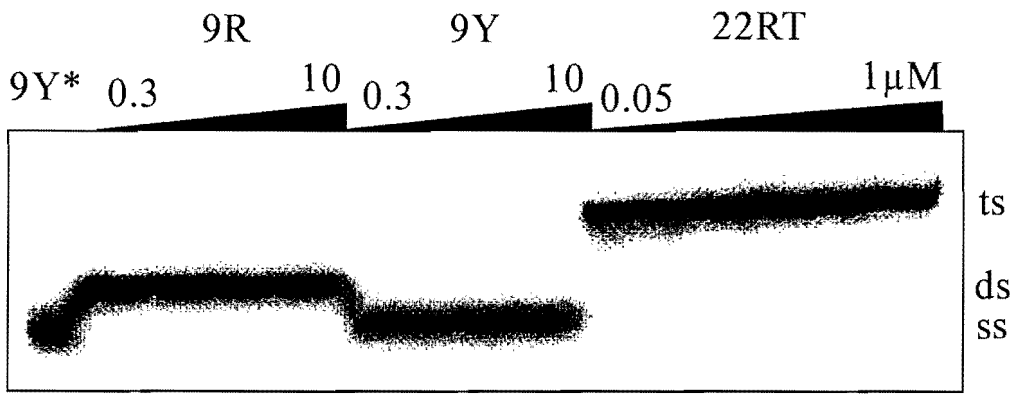

Figure 3.7.4. Scan of a 15% native PAGE of ^{32}P labelled 9mer strand alone (9Y*) with increasing concentration (0.3-10 μM) of complementary strand (9R) and 22mer ligand (22RT, 0.05-1μM) to form the duplex and purine triplex respectively. Addition of more of 9Y has no complex forming influence.

3.7.2 Influence of A for T exchange on stability of the purine triplex motif

Table 3.7.1 lists the thermodynamic data ordered according to decreasing T_m due to systematic replacement of the RHG thymines with adenine, inosine or cytosine. The trend described previously for replacing T with A for the "Limulus" structure is reproduced in this data set. It appears that an optimum stacking unit is formed when 2 T's nearest the loop are replaced by A's. The drop in stability with further substitution may indicate distortion of the underlying Watson-Crick duplex. In line with this explanation is the observation that the T_m is 4°C lower for 2 T's replaced furthest from the loop (9Y/22RA$_{7,8}$) than for two T's replaced closer to the loop (9Y/RA$_{3,5}$). To further explore the impact of the 2 T's closest to the loop on the stability they were replaced consecutively by either inosine or a cytosine mismatch.

3.7.3. Influence of I for T or A exchange on the stability of the reference purine triplex

According to Table 3.7.1 and Figure 3.7.5 replacing one or two thymines with inosine has hardly any effect on the T_m or van't Hoff enthalpy of the unfolding of the triplex motif. This is a surprising result as one would expect to lose a hydrogen bond when presenting inosine in the Reverse-Hoogsteen orientation. Nevertheless inosine can be accommodated in this position. It's influence, however, can be seen as negative when replacing adenine. There is a drop in T_m of 3.7°C on replacing an A-AT triad for an I-AT triad. Accordingly there is a drop of 6.6°C for replacing 2A's with 2I's.

Table 3.7.1: Thermodynamic data for purine motif triplexes with mutations in the Reverse Hoogsteen Strand ranked according to melting temperature (T_m) in the presence of 100mM LiAc, 20mM $MgAc_2$, 20mM NaCacodylate at pH 6.0.

Ligand Name	Reverse Hoogsteen Strand 5′ to 3′	T_m[a] (°C)	δT[b] (°C)	$-\Delta H_{vH}$ (kcal/mol)
$22RA_{3,5}$	. . . GG**A**G**A**GTTG	45.7	20.0	61
$22RA_5$	. . . GGTG**A**GTTG	43.5	18.5	65
$22RA_{3,5,7}$	. . . GG**A**G**A**G**A**TG	42.0	20.0	60
$22RA_{7,8}$	. . . GGTGTG**AA**G	41.4	23.0	52
22RA	. . . GG**A**G**A**G**AA**G	40.0	21.0	56
$22RI_5$	. . . GGTG**I**GTTG	39.8	19.5	60
$22RI_{3,5}$	. . . GG**I**G**I**GTTG	39.1	19.5	60
22RT	. . . GGTGTGTTG	38.3	19.0	61
$22RC_5$	. . . GGTG**C**GTTG	35.8	23.5	49
9R	GAAGAGAGG	35.2	18.5	62

[a] Uncertainties in T_m and ΔH values are estimated at 0.5°C and 10% respectively.

[b] δT is the melting range

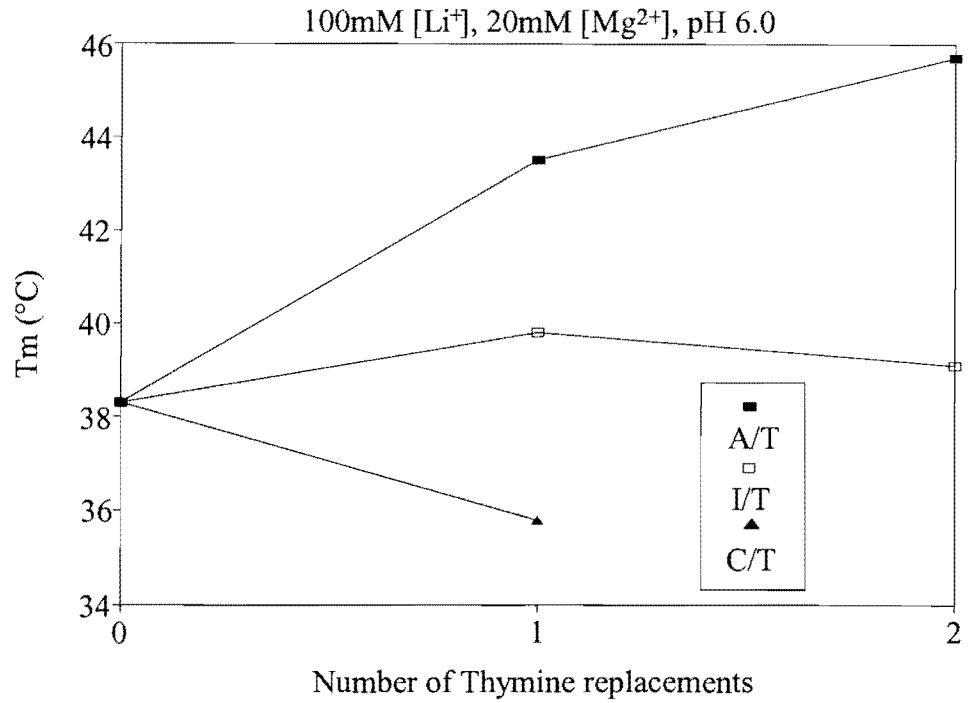

Figure 3.7.5 Comparing stability's of the purine triplex with G/T third strand sequence (9Y/22RT) with mutations of one or two Thymines exchanged for either Adenine, Inosine or Cytosine.

3.7.4 Effect of exchanging T and A for C on triplex stability

Cytosine has to be considered a mismatch in the Hoogsteen position of this complex as it does not hydrogen-bond within the purine motif at all. This is evident with a drop in T_m of 2.5°C and a reduction in ΔH_{vH} of 12 Kcal/mol for replacing a single T. Replacing an A with C drops the T_m by 7.7°C and decreases ΔH_{vH} by 16 Kcal/mol. A single C-AT mismatch is even 4°C less stable than an I-AT triad.

Table 3.7.2: The influence of loop position on the stability of a purine triple helix.

Name	Complex	T_m[a] (°C)	$\frac{dT_m}{d\log[Mg^{2+}]}$ (°C)	$-\Delta H_{vH}$ (kcal/mol)	$-\Delta S_{vH}$ (cal/mol K)	$-\Delta G_{vH,\ 37°C}$ (kcal/mol)
[a]	5′ GTGGTGGGTGGT . . . . . . 5′ CTCCTCCCTCCT | | | | | | | | | | | | GAGGAGGGAGGA	70.7	-	-	-	23.4
[a]	GTGGTGGGTGGT . . . . . . 5′CTCCTCCCTCCT | | | | | | | | | | | | GAGGAGGGAGGA 5′	69.3	-	-	-	19.9
[b]	22RA 5′GAAGAGAGG . . . . . . $9Y_{INV}$ 5′CTTCTCTCC | | | | | | | | | GAAGAGAGG	45.2	6.7 ±0.1	77.4	216	10.4
[b]	22RA GGAGAGAGG . . . . . . 9Y 5′CCTCTCTCC | | | | | | | | | GGAGAGAGG 5′	42.9	6.2 ±0.2	75.5	212	9.7
[b]	9Y 5′CCTCTCTTC | | | | | | | | | 9R GGAGAGAAG 5′	40.0	2.2 ±0.1	85.5	214	19.1

[a] Buffer: 100mM NaCl, 10mM $MgCl_2$, 10mM Na-PIPES (pH 7.0), 1.5μM strands, loop sequence (TT), (Vo et al., 1995).

[b] Buffer: 100mM LiAc, 20mM $MgAc_2$, 20mM Tris-Ac (pH 7.0), 2.5μM strands, loop (CCTT). Watson-Crick H-bonding (|);Reverse-Hoogsteen H- bonding (.)

3.7.5 The influence of loop position on triplex stability

The palindromic sequence 22RA can form a triplex with the loop connecting the purine sequences on the 3′ side of $9Y_{INV}$ or the 5′ side of 9Y due to the asymmetric nature of the sequences. Table 3.7.2 ranks the triplexes and the corresponding duplex according to T_m. It shows that the loop spanning the 3′ side of the pyrimidine strand is preferred over the loop spanning the 5′ side. This has also been observed by Vo *et al.* (1995). This is an interesting result as the purine "Limulus" might form a competing dumbbell structure with 22RA binding to both the 5′ and 3′ ends of 22Y.

The two triplexes above are isomers of one another. Why one should be preferred over the other is not obvious. This observation is called the "isomer paradox" first described for H-DNA formation (Htun & Dahlberg, 1989). The two isomers are conventionally labelled H-y3 for a 5′ loop and H-y5 for 3′ loop. It was demonstrated that G, C rich sequences at the dyad within H-DNA and/or divalent cations caused a preference for the H-y5 isomer; whereas A, T rich sequences and monovalent ions favoured H-y3 formation (Shimizu et al., 1993). The results imply that, a) the nucleation event is a determining factor for the choice of isomer, and b) the nucleation mechanisms are different for the two isomers with "denaturation or distortion of the helix being necessary for H-y3 formation to a greater extent than in the H-y5 case" (Roberts & Crothers, 1996).

Thermodynamic and modelling studies of oligonucleotide systems in the pyrimidine motif show the two isomers have similar stability's (Booher et al., 1994; Wang et al.,

1994, Roberts & Crothers, 1996). In contrast kinetic studies show that the y3 isomer of a 12-mer folds tenfold faster than the y5 isomer (Roberts & Crothers, 1996) i.e. for the pyrimidine motif the third strand "zippers" onto the duplex more quickly in the 5′ to 3′ direction. This kinetic study was possible because of the properties of class 2 triplexes in the pyrimidine motif. As described previously the binding of a pyrimidine third strand is accompanied by a significant hypochromic shift in absorbance compared to a purine third strand. The pyrimidine motif is pH dependent and so the kinetic reaction can be started by lowering the pH of a pre-equilibrated duplex-with-tail and monitored for about 200 milliseconds by absorbance-detected stopped-flow (Roberts & Crothers, 1996).

It is premature to apply these findings directly to the purine motif due to the complication of the requirement for divalent cations and more work is required in this area. Another property of the pyrimidine motif is the biphasic melting behaviour observed over a particular pH range. This property is exploited in the next chapter to further characterise the folding pathway of the "pyrimidine Limulus" and the related control triplex.

3.8 Characterisation of the pyrimidine motif in the absence of Mg^{2+}

3.8.1 Biphasic melting behaviour at pH 7.0

On construction of a phase diagram (T_m vs pH) for a pyrimidine triplex it is possible to observe a biphasic melting profile within a very small pH range (Völker *et al.* 1993; Hüsler & Klump 1995a; Plum & Breslauer, 1995; Mills et al., 1996). The first transition is assigned to the co-operative dissociation of the third strand and the second to the residual duplex melting.

The following set of melting profiles are included to completely describe the folding pathway as shown again in Figure 3.8.1. Figure 3.8.2A is a melting profile recorded at 260nm and 295nm respectively for the "Limulus" structure at pH 7.0. The biphasic nature of the profile is shown more clearly on the first derivative of the original curve Fig. 3.8.2B. The hypochromism at 295nm (inverted for the derivative plot) coincides with the first transition indicating there is a change in environment of cytosines which are located in the Hoogsteen strand. The control pyrimidine triplex gives a similar set of profiles which confirms that the "Limulus" is behaving like a pyrimidine triplex under these conditions (Figure 3.8.3A, B).

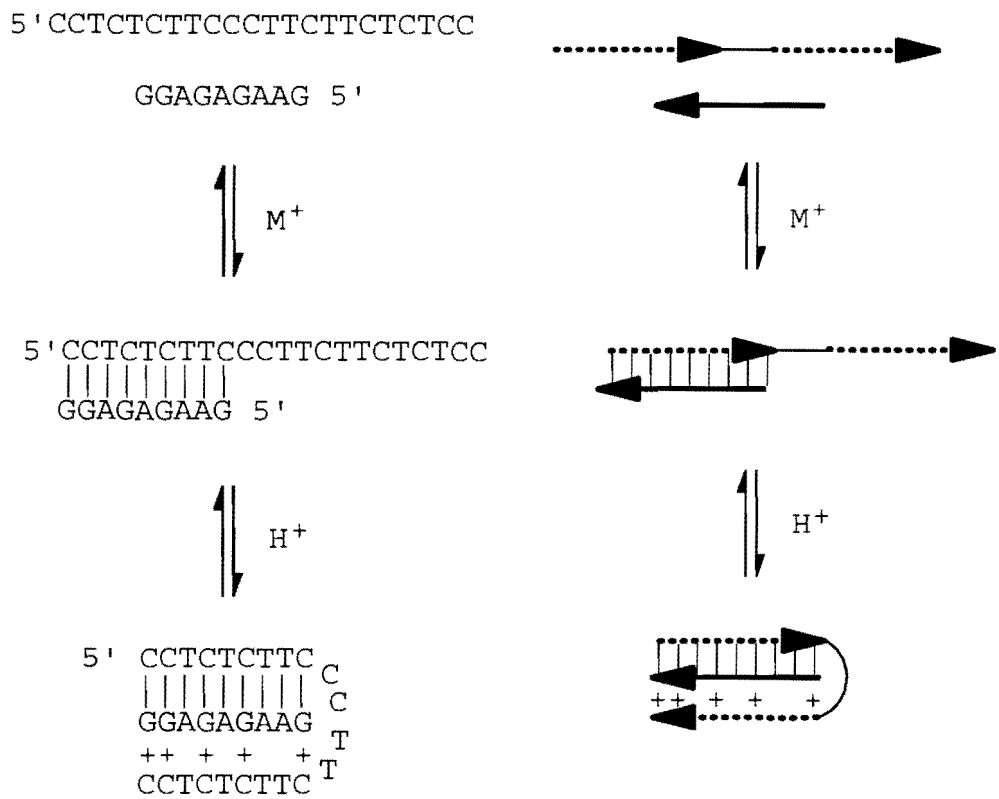

Figure 3.8.1. Proposed folding pathway for the formation of a triple helix based on the pyrimidine motif.

A

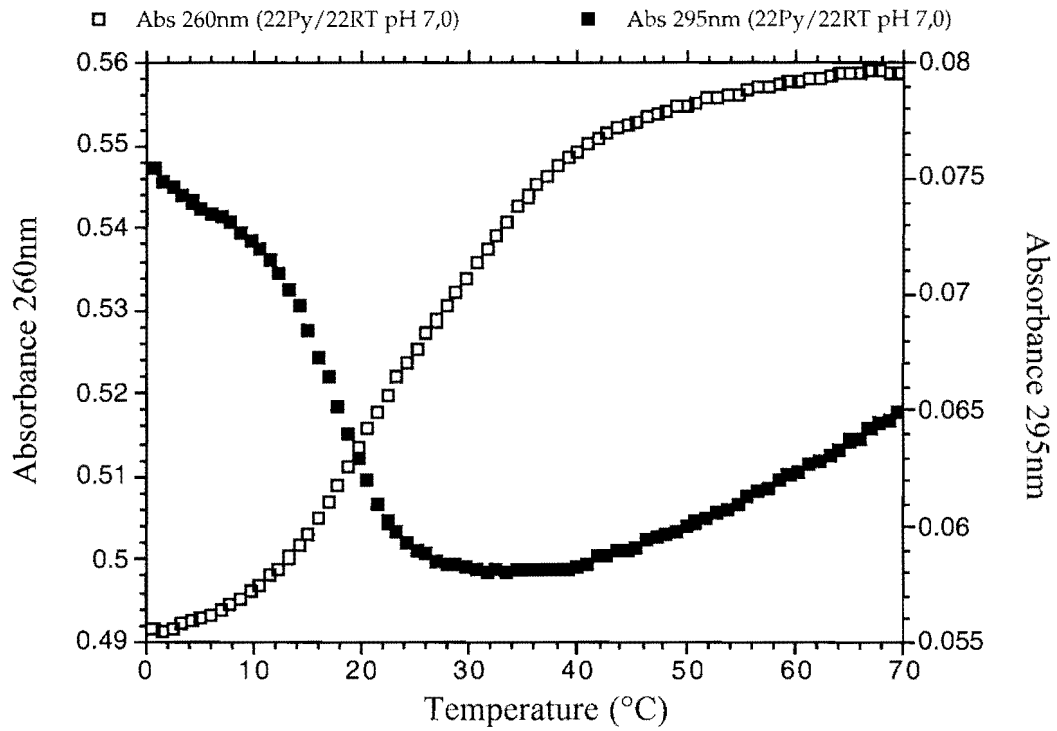

B

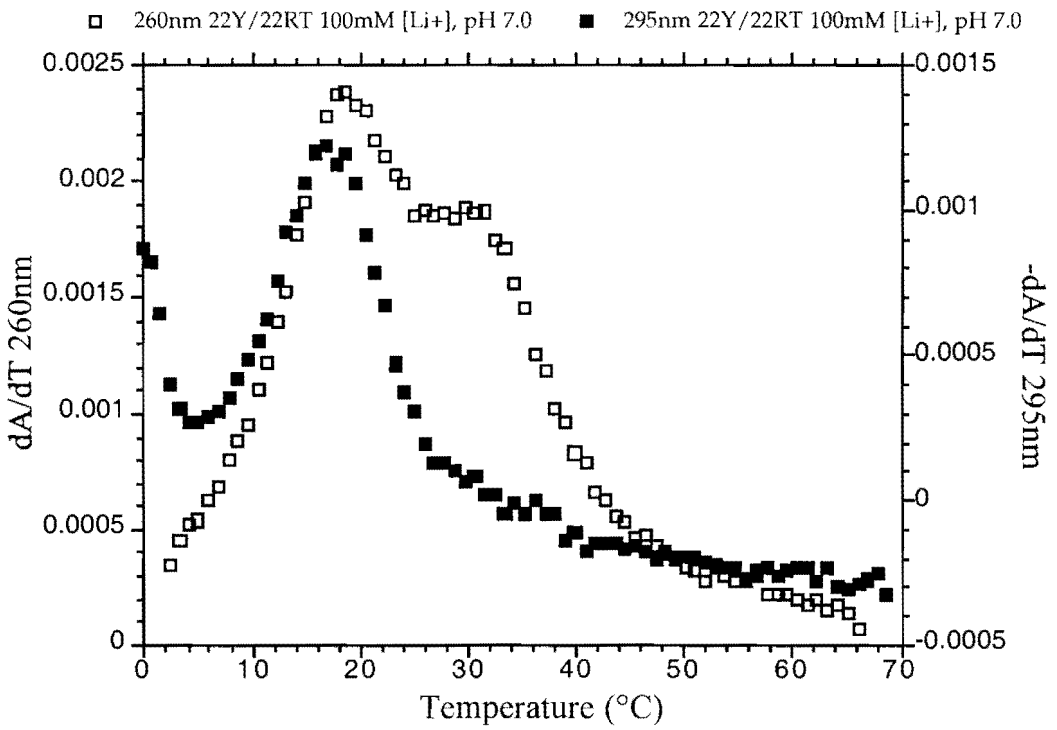

Figure 3.8.2A, Melting profiles of complex (22Y/22RT) and B, the derivative melting curves at pH 7.0, 100mM [Li^+] reveal biphasic melting behaviour in the absence of Mg^{2+}.

A

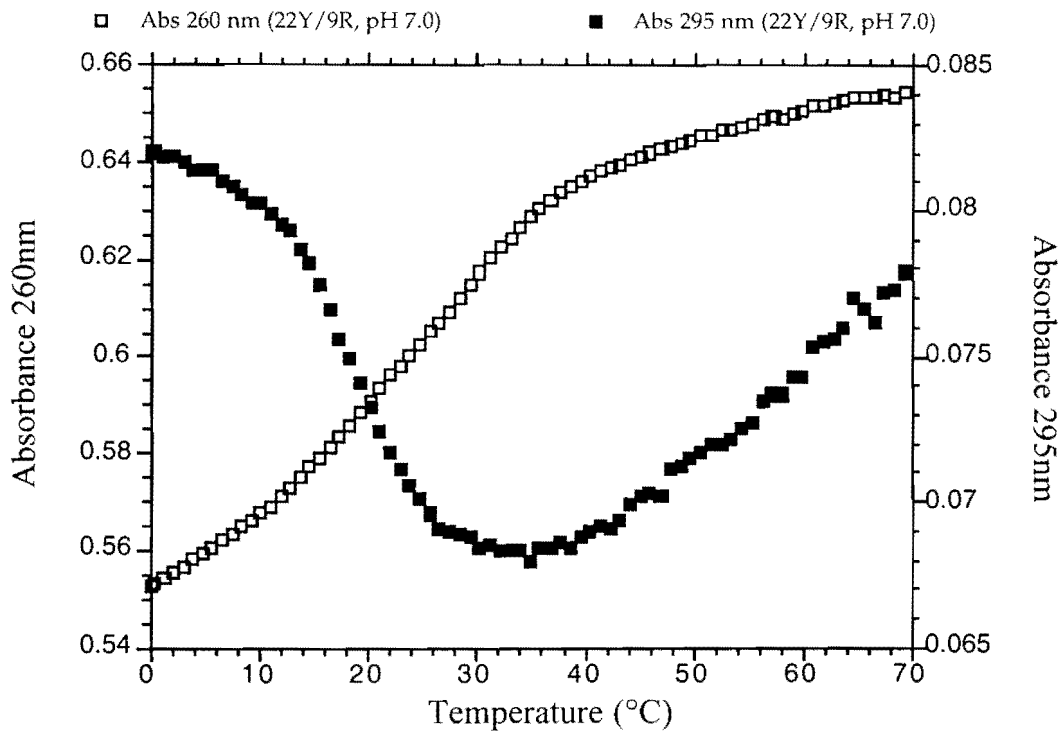

B

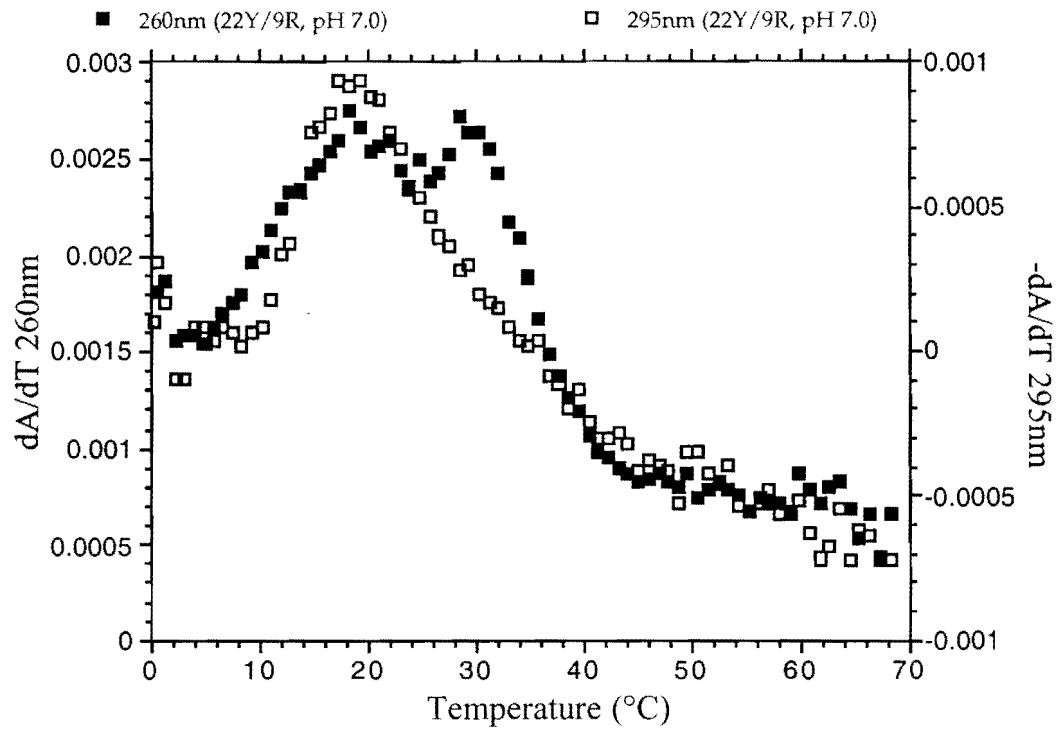

Figure 3.8.3A, Melting profiles of control pyrimidine triplex (22Y/9R) and B, the derivative melting curves at pH 7.0, 100mM [Li^+] reveal biphasic melting behaviour in the absence of Mg^{2+}.

3.8.2 Monophasic melting behaviour at pH 6.0

Figures 3.8.4 and 3.8.5 show the melting profiles and their first derivatives for the "Limulus" and the corresponding control triplex respectively at pH 6.0. On lowering the pH the triplex-duplex and duplex-coil transitions merge as the triplex becomes more stabilised relative to the duplex. The melting profile becomes monophasic and the T_m's of the curves recorded at 260nm and 295nm coincide describing a single triplex-coil transition. The two triplex structures behave similarly and once again confirm the "Limulus structure" is represented by the pyrimidine motif under these conditions (absence of Mg^{2+}).

A

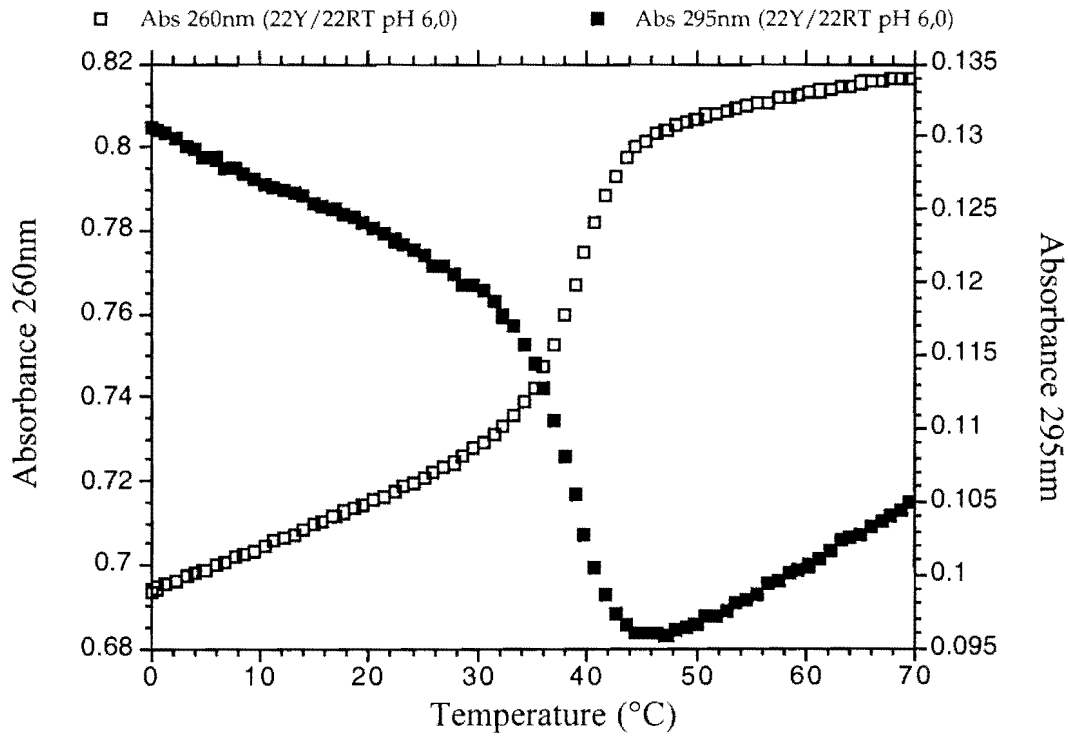

B

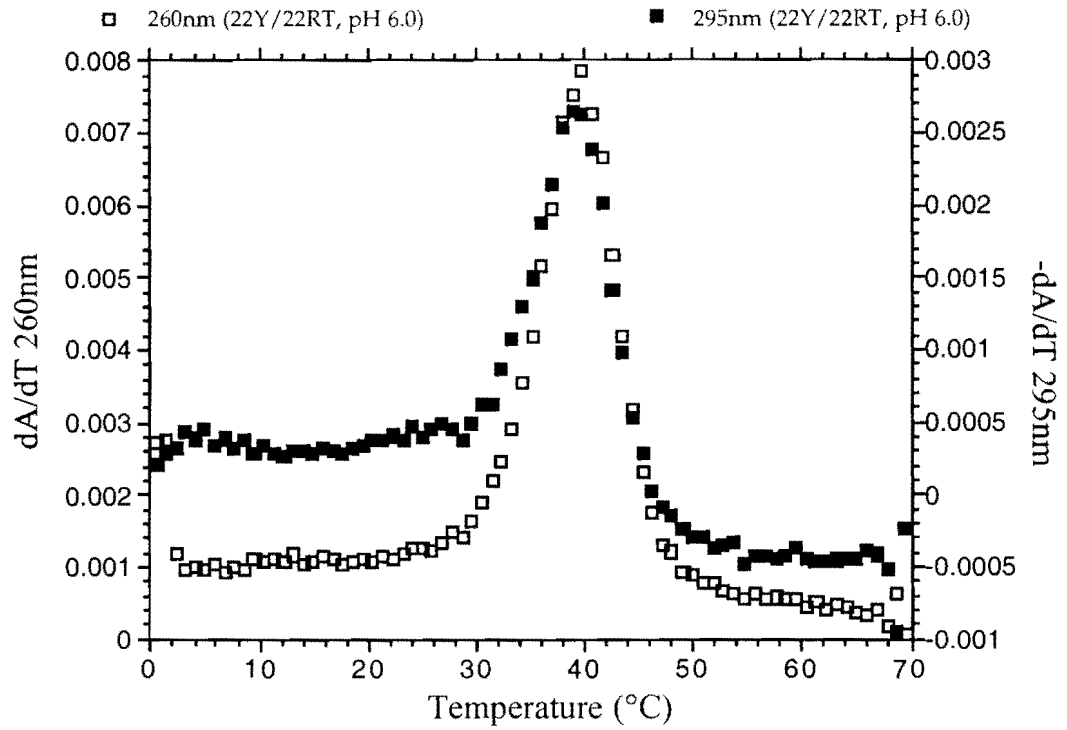

Figure 3.8.4 Melting profiles of A, complex (22Y/22RT) and B, the derivative melting profiles at pH 6.0, 100mM [Li^+]. The T_m's coincide with monophasic melting behaviour. This profile represents the triplex to coil transition.

A

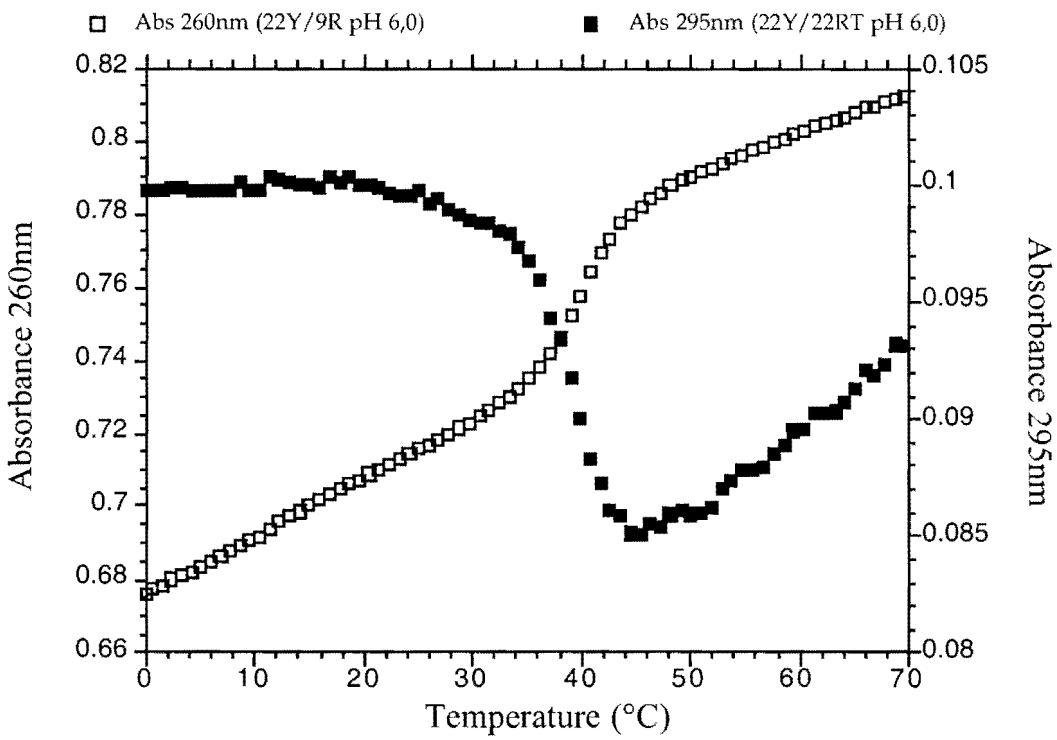

B

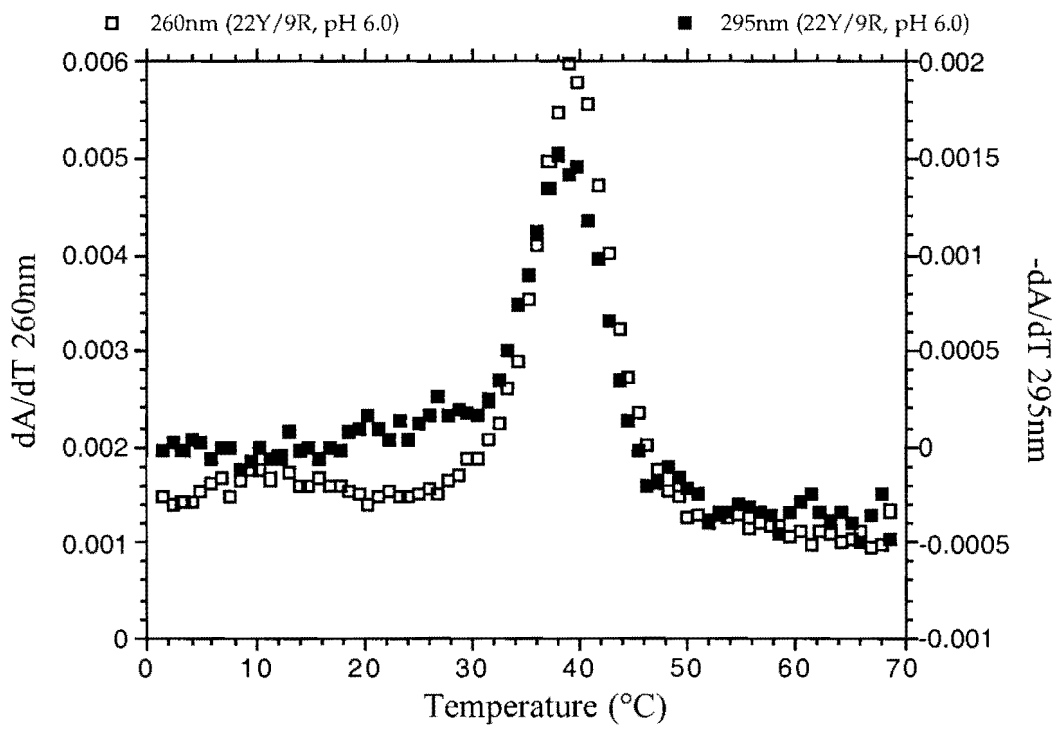

Figure 3.8.5A, Melting profiles of control pyrimidine triplex (22Y/9R) and B, the monophasic derivative melting curves at pH 6.0, 100mM [Li^+] in the absence of Mg^{2+}.

Conclusion

Results of a thermodynamic characterisation of the "Limulus structure" show that the purine- and pyrimidine-motif single strand extensions can compete for the same core Watson-Crick duplex resulting in either a purine or pyrimidine motif triplex. This competition is revealed in a phase diagram, a plot of melting temperature (T_m) versus pH. The Limulus structure consists of two 22-mer strands of oligodeoxynucleotides which overlap in the presence of monovalent ions to form a core 9-mer WC duplex with a 3′ extension on either end. On lowering the pH from neutral the extension consisting of C and T (Hoogsteen strand) folds onto the duplex to form a pyrimidine-motif triplex with 3′ purine single strand extension. On addition of divalent cations (Mg^{2+}) at neutral pH the extension consisting of G and T (reverse-Hoogsteen strand) folds onto the WC duplex forming the purine-motif triplex with 3′ pyrimidine single strand extension. Above pH 6.1 and in the presence of 20mM Mg^{2+} the Purine Limulus is favoured over the Pyrimidine Limulus and the converse is true below pH 6.1 and in the absence of Mg^{2+}.

It can be demonstrated, using the Limulus structure, that the two triplex motifs can also be interchanged by changing the magnesium concentration at a fixed pH value. Mg^{2+} stabilises the purine motif to a greater extent than the pyrimidine motif since the pyrimidine motif is already partially stabilised by the formal positive charges on the cytosines.

DNA triplexes in the purine motif can accommodate the A-AT triad as well as the T-AT and G-GC triads. Systematic substitution of T for A in the reverse-Hoogsteen extension of the Limulus structure reveals a concomitant increase in stability (melting temperature) of the Purine Limulus until 3 out of 4 T's are replaced by A. This is attributed to an increase in stacking interaction gained by introducing the larger purine base. Substitution of all 4 T's with A makes the purine-rich strand into a palindrome which can form a competing structure and the trend of increasing stability is no longer observed. The stability of the Pyrimidine Limulus is unaffected by the mutations as expected. The increase in stability can be described as linear when one plots the T_m at the triple-point of the phase diagram versus the number of T's replaced by A's.

The Limulus structure behaves similarly to the underlying triplexes which are also characterised along with the core duplex for comparison. By systematically replacing T's with A's in the reversed-Hoogsteen strand of the control purine triplex there is an increase in T_m until half of the third strand, actually the sequence closest to the loop, consists of purines. Further substitution in the other half of the third strand lowers the stability of the triplex again. This may be due to distortion of the underlying Watson-Crick double helix. The Limulus structure can accommodate up to 3 replacements and still maintain the trend of increased stability by introducing more purines into the third strand. This is attributed to the fact that it is not blunt ended and may gain some stacking interaction reaching into the 3′ extension.

Systematic mutations incorporating inosine and cytosine into the third strand sequence closest to the loop of the control purine triplex reveal that the triads can be ranked according to the stability of the resulting triplex indicated by T_m in the following order: A-AT > T-AT = I-AT > C-AT where C is considered a mismatch.

References

Anderson, C.F. & Record, T.M.Jr (1982)

Polyelectrolyte theories and their applications to DNA.

Ann. Rev. Phys. Chem. 33, 191-222

Arnott, S & Bond, P. (1973)

Triple-Stranded Polynucleotide Helix Containing Only Purine Bases.

Science. 181, 68-69

Arnott, S & Selsing, E. (1974)

Structures for the polynucleotide complexes poly(dA)·poly(dT) and poly(dT)·poly(dA)·poly(dT).

J. Mol. Biol. 88, 509-521

Beal, P.A. & Dervan, P.B. (1991)

Second structural motif for recognition of DNA by oligonucleotide directed triple helix formation.

Science 251, 1360-63

Beal, P.A. & Dervan, P.B. (1992)

The influence of single base triplet changes on the stability of a Pur.Pur.Pyr triple helix determined by affinity cleaving.

Nucleic Acids Res. 20, 2773-2776

Berressem, R. & Engels, J.W. (1995)

6-oxocytidine a novel protonated C-base analogue for stable triple helix formation.

Nucleic Acids Res. 23, 3465-3472

Booher, M.A., Wang, S. & Kool, E.T. (1994)
Base-pairing and steric interactions between pyrimidine strand bridging loops and the purine strand in DNA pyrimidine.purine.pyrimidine triplexes.
Biochemistry 33, 4645-4651

Breslauer, K.J., Frank, R., Blöcker, H. & Marky, L.A. (1986)
Predicting DNA duplex stability from the base sequence.
Proc. Natl. Acad. Sci. USA 83, 3746-3750

Case-Green, S.C. & Southern, E.M. (1994)
Studies on the base pairing properties of deoxyinosine by solid phase hybridisation to oligonucleotides.
Nucleic Acids Research, 22, 131-136

Cantor, C.R., & Schimmel, P.R. (1980)
Biophysical Chemistry Vol.1, San Fransisco: Freeman

Chan, P. P. & Glazer, P. M. (1997)
Triplex DNA: fundamentals, advances, and potential applications for gene therapy.
J Mol Med 75, 267-282

Chen, F-M (1991)
Intramolecular Triplex Formation of the Purine-Purine-Pyrimidine Type.
Biochemistry 30, 4472-4479

Cheng, A.J. & Van Dyke, M.W. (1993)
Monovalent cation effects on intermolecular purine-purine-pyrimidine triple-helix formation.
Nucleic Acids Research 21, 5630-5635

Cheng, A.J. & Van Dyke, M.W. (1994)
Oligodeoxyribonucleotide length and sequence effects on intermolecular purine-purine-pyrimidine triple-helix formation.
Nucleic Acids Research 22, 4742-4747

Cheng, Y.K. & Pettitt, B.M. (1992)
Stability's of double- and triple-strand helical nucleic acids.
Prog. Biophys. Mol. Biol 58, 225-2257.

Cherny, D.I., Malkov, V.A., Volodin, A.A. & Frank-Kamenetskii (1993)
Electron microscopy visualisation of oligonucleotide binding to duplex DNA via triple helix formation.
J. Mol. Biol. 230, 379-383

Cooney, M., Czernuszewicz, G., Postel, E.H., Flint, S.J., & Hogan, M.E. (1988)
Site-specific oligonucleotide binding represses transcription of the human *c-myc* gene in vitro.
Science, 241, 456-459

Corfield , P.W.R., Hunter, W.N., Brown, T., Robinson, P., Kennard, O. (1987)
Inosine.adenine base pairs in a B-DNA duplex.
Nucleic Acids Research, 15, 7935-7949

de Bizemont, T, Duval-Valentin, G, Sun, J. S., Bisagni, E, Garéstier T. &
Hélène, C. (1996)
Alternate strand recognition of double-helical DNA by (T,G)-containing oligonucleotides in the presence of a triple helix-specific ligand.
Nucleic Acids Res, 24, 1136-1143

de los Santos, C., Rosen, M. & Patel, D (1989)
NMR studies of DNA $(R+)_n$ $(Y-)_n$ $(Y+)_n$ triple helices in solution: immino and amiino proton markers of T-AT and C+-GC base triple formation.
Biochemistry 28, 7282-7289

Durland, R.H., Kessler, D.J., Gunnell, S., Duvic, M., Pettitt, B.M.
& Hogan, M.E. (1991)
Binding of triple helix forming oligonucleotides to sites in gene promoters.
Biochemistry 30, 9246-9255

Duval-Valentin, G., Thoung, N.T., & Hélène, C. (1992)
Specific inhibition of transcription by triple helix-forming oligonucleotides.
Proc. Natl. Acad. Sci. USA, 89, 504-508

Ebbinghaus, S.W., Gee, J.E., Rodu, B., Mayfield, C.A., Sanders, G. & Miller, D.M. (1993). Triplex formation inhibits HER-2/*neu* transcription in vitro.
J. Clin. Invest. 92, 2433-2439

Egholm, M., Nielson, P.E., Buchard, O. & Berg, R.H. (1992)
Recognition of guanine and adenine in DNA by cytosine and thymine containing peptide nucleic acids (PNA).

Faucon, B., Mergny J. L. & Hélène C. (1996)
Effect of third strand composition on the triple helix formation: purine versus pyrimidine oligodeoxynucleotides.
Nucleic Acids Res 24, 3181-3188

Felsenfeld, G., Davies, D.R., & Rich, A. (1957)
Formation of a three stranded polynucleotide molecule.
J. Am. Chem. Soc. 79, 2023-2024

Frank-Kamenetskii, M.D., Malkov, V.A., Voloshin, O.N. & Soyfer, V.N. (1991)
Stabilisation of PyPuPu triplexes with bivalent cations.
Nucleic Acids Res. Symp. Ser. 24, 159-162

Frank-Kamenetskii, M.D. & Mirkin, S.M. (1995)
Triplex DNA Structures.
Annu. Rev. Biochem. 64, 65-95

Francois, J.C., Saison-Behmoaras, T., Thuong, N.T. & Hélène, C. (1989)
Inhibition of restriction endonuclease cleavage via triple helix formation by homopyrimidine oligonucleotides.
Biochemistry 28, 9617-9619

Fresco. J.R. & Klemperer, E. (1959)
Polyriboadenylic acid, a molecular analogue of ribonucleic acid and deoxyribonucleic acid.
Ann. N.Y. Acad. Sci. 81, 730-741

Fresco. J.R. & Massoulie J. (1963)
Polynucleotides .v. helix-coil transition of polyriboguanylic acid.
J. Amer. Chem. Soc. 85, 1352

Gee, J.E., Blume, S., Snyder, R.C., Ray, R. & Miller (1992)
Triplex formation prevents Sp1 binding to the dihydropholate reductase promoter.
J. Biol. Chem. 267, 11163-11167

Griffin, L.C. & Dervan, P.B. (1989)
Recognition of Thymine.Adenine Base Pairs by Guanine in a Pyrimidine Triple Helix Motif.
Science, 245, 967- 971

Grigoriev, M., Praseuth, D., Robin, P., Hemar, A., Saison-Behmoaras, T., Dautry-Varsat, A., Thuong, N.T., Hélène, C. & Harrel-Ballan (1992)
A triple helix forming oligonucleotide intercalator conjugate acts as a transcriptional repressor via inhibition of NFκB binding to interleukin-2 receptor α-regulatory sequence.
J. Biol. Chem. 267, 3389-3395

Grigoriev, M., Praseuth, D., Guyesse, A.L., Robin, Thuong, N.T., Hélène, C. & Harrel-Ballan (1993)
Inhibition of gene expression by triple helix directed DNA cross-linking at specific genes.
Proc. Nat. Acad. Sci. USA 90, 3501-3505

Häner, R. & Dervan, P.B. (1990)
Single-stranded DNA Triple-Helix formation.
Biochemistry, 29, 9761-9765

Havre, P.A., Gunther, E.J., Gasparro, F.P. & Glazer, P.M. (1993)
Targeted mutagenesis of DNA using triple helix-forming oligonucleotides linked to psoralen.
Proc. Natl. Acad. Sci. USA. 90, 7879-7883

Hélène, C., Thuong, N.T., Saison-Behmoaras, T. & Francois, J.C. (1989)
Sequence-specific artificial endonucleases.
Trends Biotechnol. **7**, 310-315

Hélène, C., Thuong, N.T. & Harrel-Bellan (1992)
Control of gene expression by triple helix-forming oligonucleotides. The antigene strategy.
Ann. NY Acad. Sci. 660, 27-36

Hoogsteen, K. (1959)
The structure of crystals containing a hydrogen-bonded complex of 1-methylthymine and 9-methyladenine.
Acta crystallogr. 12, 822-823

Htun, H & Dahlberg, J.E. 1989
The structure and formation of triple-stranded H-DNA
Science 243, 1571-1576

Hüsler, P.L. & Klump, H.H. (1994)
Unfolding of a Branched Double-Helical DNA Three-way Junction with Triple-Helical Ends.
Archives of Biochemistry and Biophysics 313, 29-38

Hüsler, P.L. & Klump, H.H. (1995a)
Thermodynamic characterisation of a Triple Helical Three-way junction containing a Hoogsteen branch point.
Archives of Biochemistry and Biophysics 322, 149-166

Hüsler, P.L. & Klump, H.H. (1995b)
Prediction of pH-Dependent Properties of DNA Triple Helices.
Archives of Biochemistry and Biophysics 317, 46-56

Imagawa, S., Izumi, T. & Miura, Y. (1994)
Positive and negative regulation of erythropoietin gene.
J. Biol. Chem. 269, 9038-9044

Ing, N.H., Beekman, J.M., Kessler, D.J., Murphy, M., Jayaraman, K., Zendegui, J.G., Hogan, M.E., O'Malley, B.W. & Tsai, M.J. (1993)
In vivo transcription of a progesterone-responsive gene is specifically inhibited by a triple-forming oligonucleotide.
Nucl. Acids Res. 21, 2789-2796

Ito, T., Smith, C.L. & Cantor, C.R. (1992a)
Sequence-specific DNA purification by triplex affinity capture.
Proc. Natl. Acad. Sci. USA. 89, 495-498

Ito, T., Smith, C.L. & Cantor, C.R. (1992b)
Affinity capture electrophoresis for sequence-specific DNA purification.
Genet. Anal. Techi. Appl. 9, 96-99

Ito, T., Smith, C.L. & Cantor, C.R. (1992c)
Triplex affinity capture of a single copy clone from a yeast genomic library.
Nucleic Acids Research 20, 3524

Johnson, K.H., Durland, H.R., Hogan, M.E. (1992)
The vacuum UV CD spectra of G.G.C triplexes.
Nucleic Acids Research 20, 3859-3864

Johnson, K. H., Grav, D.M. & Sutherland, J.C. (1991)
Vacuum UV CD spectra of homopolymer duplexes and triplexes containing A-T or A-U basepairs.
Nucleic Acids Research 19, 2275-2280

Kandimalla, E.R. & Agrawal, S. (1994)
Single-strand-targeted triplex formation: stability, specificity and RNAse H activation.
Gene 149, 115-121

Kiyama, R., Nishikawa, N. & Oishi, M. (1994)
Enrichment of human DNAs that flak poly(dA)-poly(dT) tracts by DNA triplex formation.
J. Mol. Biol. 273, 193-200

Klump, H.H. (1987)
Energetics of order/order transitions in nucleic acids.
Can. J. Chem., 66, 804-811

Klump, H.H. (1988).
Conformational transitions in nucleic acids.
In *Biochemical Thermodynamics* (Jones, M. N., ed.), 2nd edit., pp. 100-144, Elsevier.

Kohwi, Y. & Kohwi-Shigematsu, T. (1988)
Magnesium ion-dependent triple-helix structure formed by homopurine-homopyrimidine sequences in supercoiled plasmid DNA.
Proc. Natl. Acad. Sci. USA 85, 3781-3785

Kohwi, Y. & Kohwi-Shigematsu, T. (1993)
Structural Polymorphism of homopurine-hompyrimidine sequences at neutral pH.
J. Mol. Biol. 231, 1090-1101

Kool, E.T. (1991)
Molecular recognition by circular oligonucleotides: increasing the selectivity of DNA binding.
J. Am. Chem. Soc. 113, 6265-6266

Le Doan, T.. Perrouaulat, L., Praseuth, N., Habhoub, N., Decoult, J.L., Thuong, N.T., Lhomme, J. & Hélène, C. (1987)
Sequence specific recognition, photocross- linking, and cleavage of the DNA double-helix by an oligo-[a]-thymidilate covalently linked to an azidoproflavine derivative.
Nucleic Acids. Res. 15, 7749-7760

Lee, J.S., Woodsworth, M.L., Latimer, L.J. & Morgan, A.R. (1984)
Poly(pyrimidine) poly(purine) synthetic DNA containing 5-methylcytosine form stable triplexes at neutral pH.
Nucleic Acids. Res. 12, 6603-6614

Letai, A.G., Palladino, M.A., Fromm, E., Rizzo, V. & Fresco, J. R. (1988).
Specificity in formation of triple stranded nucleic acid helical complexes: studies with agarose-linked polyribonucleotide affinity columns.
Biochemistry, 27, 9108-9112.

Lipset, M.N. (1964)
Complex formation between polycytidylic acid, and guanine oligonucleotides.
J. Biol. Chem. 239, 1256-1260

Lu, G. & Ferl, R.J. (1992)
Site-specific oligodeoxynucleotide binding to maize *Adh*1 gene promoter represses *Adh*1-GUS gene expression in vivo.
Plant. Mol. Biol. 19, 715-723

Luebke, K.J. & Dervan, P.B. (1991)
Nonenzymatic sequence-specific ligation of double-helical DNA.
J. Am. Chem. Soc. 113, 7447-7448

Luebke, K.J. & Dervan, P.B. (1992)
Nonenzymatic ligation of double-helical DNA by alternate-strand triple helix formation.
Nucleic Acid Res. 20, 3005-3009

Lyamichev, V.I., Mirkin, S.M. & Frank-Kamenetskii, M.D. (1986)
Structures of homopurine-homopyrimidine tract in superhelical DNA.
J. Biomol. Struct. Dyn. 3, 667-669

Maher, L.J.,III, Wold, B., & Dervan, P.B. (1989)
Inhibition of DNA binding proteins by oligonucleotide-directed triple helix formation.
Science 245, 725-730

Malkov, V.A., Voloshin, O.N., Veselkov, A.G., Rostapshov, V.M., Jansen, I., Soyfer, V.N. & Frank-Kamenetskii, M.D. (1993)
Protonated pyrimidine-purine-purine triplex.
Nucleic Acids Research 21, 105-111

Manning, G.S. (1978)
The molecular theory of polyelectrolyte solutions with applications to the electrostatic properties of polynucleotides.
Q. Rev. Biophys. 11, 179-246

Manzini, G., Xodo, L.E., Gasporotto, D., Quadrifoglio, F., van der Marel, G.A. & van Boom, J.H. (1990)
Triple Helix formation by oligopurine-oligopyrimdine DNA fragments; electrophoretic and thermodynamic behaviour.
J.Mol.Biol 213, 833-843

Mark, C., & Thiele, D. (1978)
Poly(dG).poly(dC) at neutral and alkaline pH; the formation of triple stranded poly(dG).poly(dG).poly(dC).
Nucleic Acids Res. 5, 1017-1028

Marky, L.A. & Breslauer, K.J. (1987)
Calculating Thermodynamic Data for Transitions of any Molecularity from Equilibrium Melting Curves.
Biopolymers, 26, 1601-1620

Mayfield, C, Ebbinghaus S, Gee J, Jones D, Rodu B, Squibb M, Miller D (1994)
Triplex formation by human Ha-ras promoter inhibits Sp1 binding and in vitro transcription.
J. Biol. Chem. 269, 18232-19238

McShan, W.M., Rossen, R.D., Laughter, A.H., Trial, J., Kessler, D.J., Zendegui, J.G., Hogan, M.E. & Orson, F.M. (1992)
Inhibition of transcription of HIV-1 in infected human cells by oligodeoxynucleotides designed to form DNA triple helices.
J. Biol. Chem. 267, 5712-5721

Miles. H.T. (1964)
The structure of the three-stranded helix, poly(A+2U).
Proc. Natl. Acad. Sci. USA.51, 1104-1109

Milligan, J.F., Krawczyk, S.H., Shalini, W., & Matteucci, M.D. (1993)
An anti-parallel triple helix motif with oligodeoxynucleotides containing 2'deoxyguanosine and 7-deaza-2'-deoxyxanthosine.
Nucleic Acids Res. 21, 327-333

Mills, M., Völker, J. & Klump H.H. (1996)
Triple helical structure involving inosine: There is a penalty for promiscuity.
Biochemistry 35, 13338-13344

Mills, M. & Klump H.H. (1997)
A new twist to an old tale: The influence of the exchange of thymine for adenine on the stability of a purine motif DNA triple helix.
South African Journal of Chemistry, 50(4), 184-188

Mills, M. & Klump H.H. (1998)
Systematic mutation in the third strand of a purine motif DNA triple helix.
Nucleosides and Nucleotides (in press)

Mirkin, S.M. & Frank-Kamenetskii, M.D. (1994)
H-DNA, and related structures.
Annu. Rev. Biophys. Biomol. Struct. 23, 541-576

Moores, J.C. (1990)
A new vector for rapid mapping of genomic DNA.
Strategies 3, 23-29

Morgan & Wells (1968)
Specificity of the three-stranded complex formation between double-stranded DNA, and single-stranded RNA containing repeating nucleotide sequences.
J. Mol. Biol. 37, 63-80

Moser, H.E., & Dervan, P.B. (1987)
Sequence-specific cleavage of double helical DNA by triple helix formation.
Science 238, 645-650

Mouscadet, J-F., Carteau, S., Goulaouic, H., Subra, F. & Auclair, C. (1994a)
Triplex-mediated inhibition of HIV DNA integration in vitro.
J. Biol. Chem. 269, 21635-21638

Narang, S.A. (1987)
Synthesis and applications of DNA and RNA.
Academic Press Inc., New York

Noonberg, S.B., Scott, G.K., Hunt, C.A., Hogan, M.E. & Benz, C.C. (1994)
Inhibition of transcription factor binding to the HER2 promoter by triplex-forming oligodeoxyribonucleotides.
Gene 149, 123-126

Noonberg, S.B., Francois, J-C., Garéstier, T. & Hélène, C. (1995)
Effect of competing self-structure on triplex formation with purine rich oligodeoxynucleotides containing GA repeats.
Nucleic Acids Research 23, 1956-1963

Ohms, J. & Ackermann, T (1990)
Thermodynamics of double- and triple-helical aggregates formed by self-complementary oligoribonucleotides of the type rA_xU_y.
Biochemistry 29, 5237-5244

Ojwang, J., Elaggari, A., Marshall, H.B., Jayaraman, K., McGrath, M.S. & Rando, R.F. (1994)
Inhibition of human immunodeficiency virus type 1 activity in vitro by oligonucleotides composed entirely of guanosine, and thymidine.
J. Acquired Immune Deficiency Syndromes 7, 560-570

Olivas, W.M., & Maher III, J.L. (1994)
Analysis of duplex DNA by triple helix formation: application to detection of a p53 microdeletion.
BioTechniques 16, 128-132

Olivas, W.M., & Maher III, J.L. (1995)
Competitive Triplex/Quadruplex Equilibria involving guanine-rich oligonucleotides..
Biochemistry 34, 278-284

Orson, F.M., Thomas, D.W., McShan, W.M., Kessler, D.J. & Hogan, M.E. (1991)
Oligonucleotide inhibition of IL2Rα mRNA transcription by promoter region collinear triplex formation in lymphocytes.
Nucleic Acids Research 19, 3435-3441

Pei, D., Ulrich, H.D. & Schultz, P.G. (1991)
A combinatorial approach toward DNA recognition.
Science 253, 1408-1411

Pilch, D.S., Brousseau, R. & Schafer, R.H. (1990a)
Thermodynamics of triple helix formation: spectrophotometric studies on the $d(A)_{10}.2d(T)_{10}$, and $d(C^+_3T_4C^+_3).d(G_3A_4G_3).d(C_3T_4C_3)$ triple helices.
Nucleic Acids Research 18, 5743-5750

Pilch, D.S., Levenson, C., Shafer, R.H. (1991)
Structure, stability, and thermodynamics of a short intermolecular purine-purine-pyrimidine triple helix. *Biochemistry 30*, 6081

Plum, G.E., Park, Y.W., Singleton, S.F., Dervan, P.B. & Breslauer, K.J. (1990)
Thermodynamic characterisation of the stability, and the melting behaviour of a DNA triplex: a spectroscopic, and calorimetric study.
Proc. Natl. Acad. Sci. USA 87, 9436-9440

Plum, G.E., & Breslauer, K.J. (1995a)
Thermodynamics of an Intramolecular DNA triple Helix: A Calorimetric and Spectroscopic Study of the pH and Salt Dependence of Thermally Induced Structural Transitions.
J.Mol.Biol. 248, 679-695

Plum, G.E., Park, Y.W., Singleton, S.F. & Breslauer, K.J. (1995b)
Nucleic acid hybridisation: triplex stability and energetics.
Annu. Rev. Biophys. Biomol. Struct. 24, 319-350.

Postel, E.H., Flint, S.J., Kessler, D.J. & Hogan, M.E. (1991)
Evidence that a triplex-forming oligodeoxyribonucleotide binds to the *c-myc* promoter in HeLa Cells, thereby reducing *c-myc* mRNA levels.
Proc. Natl. Acad. Sci. USA 88, 8227-8231

Povsic, T.J. & Dervan, P.B. (1989)
Triple helix formation by oligonucleotides by DNA extended to the physiological pH range.
J. Am. Chem. Soc. 111, 3059-3061

Povsic, T.J., Strobel, S.A. & Dervan, P.B. (1992)
Sequence-specific double strand alkylation, and cleavage of DNA mediated by triple helix formation.
J. Am. Chem. Soc. 114, 5934-5941

Radhakrishnan I., de los Santos, C., Patel D.J. (1991)
Nuclear Magnetic Resonance Structural Studies of Intramolecular Purine-Purine-Pyrimidine DNA triplexes in solution.
J.Mol.Biol. 221, 1403-1418

Radhakrishnan I. & Patel, D.J. (1993a)
Solution structure of an intramolecular purine-purine-pyrimidine DNA triplex.
J. Am. Chem. Soc. 115, 1615-1617

Radhakrishnan I. & Patel, D.J. (1993b)
Solution structure of an purine-purine-pyrimidine DNA triplex containing G-GC and T-AT triples.
Structure 1, 135-152

Radhakrishnan I. & Patel, D.J. (1994a)
Solution Structure and Hydration Patterns of a Pyrimidine.purine.pyrimidine DNA Triplex containing a novel T.GC Base-triple.
J.Mol.Biol. 241, 600-619

Radhakrishnan, I. & Patel D, J. (1994b)
DNA Triplexes: Solution Structures, Hydration Sites, Energetics, Interactions, and Function.
Biochemistry, 33, 11405-11416.

Rajagopal, P. & Feigon, J. (1989a)
Triple stranded formation in the homopurine: homopyrimidine DNA oligonucleotides $d(G\text{-}A)_4$ and $d(T\text{-}C)_4$.
Nature 339, 637-640

Rajagopal, P. & Feigon, J. (1989b)
NMR studies of triple strand formation from the homopurine-homopyrimidine deoxyribonucleotides $d(GA)_4$ and $(TC)_4$.
Biochemistry 28, 7859-7870

Rich, A (1958)
Formation of two-, and three stranded helical molecules by polyinosinic acid, and polyadenylic acid.
Nature 181, 521-525

Roberts, R.W. & Crothers, D.M. (1991)
Specificity and stringency in DNA triplex formation.
Proc. Natl. Acad. Sci. USA. 88, 9397-9401

Roberts, R.W. & Crothers, D.M, (1992)
Stability and properties of double and triple helices: dramatic effects of RNA or DNA backbone composition.
Science, *258*, 1463-1466

Roberts, R.W. & Crothers, D.M. (1996)
Kinetic discrimination in the folding of intramolecular triple helices.
J. Mol. Biol. 260, 135-146

Ross, C., Samuel, M. & Broitman, S.L. (1992)
Transcription inhibition of the bacteriophage T7 early promoter region by oligonucleotide triple helix formation.
Biochem. Biophys. Res. Common. 189, 1674-1680

Rougée, M., Faucon, B., Mergny, J.L., Barcelo, F., Giovannangéli, Garestier, T. & Hélène (1992)
Kinetics and thermodynamics of triple-helix formation: effects of ionic strength and mismatches.
Biochemistry 31, 9269-9278

Roy, C. (1993)
Inhibition of gene transcription by purine rich triplex forming oligodeoxyribonucleotides.
Nucleic Acids Res 21, 2845-2852

Roy, C. (1994)
Triplex-helix formation interferes with the transcription, and hinged DNA structure of the interferon-inducible 6-16 gene promoter.
Eur. J. Biochem. 220, 493-503

Scaggiante, B., Morassuti, G., Tolazzi, G., Michelutti, A., Baccarani, M & Quadrifoglio, F. (1994)
Effect of unmodified triple helix-forming oligodeoxyribonucleotide targeted human multidrug-resistance gene *mdr*1 in MDR cancer cells.
FEBS Lett. 352, 380-384

Scaria, P.V. & Schafer, R.H. (1991)
Binding of ethidium bromide to a DNA triple helix: evidence for intercalation.
J.Biol.Chem. 266, 5417-5423

Scaria, P.V., Shire, S.F. & Schafer, R.H. (1992)
Quadruplex structure of ($G_2T_4G_4$) stabilised by K^+ or Na^+ is an asymmetric hairpin dimer.
Proc. Natl. Acad. Sci. USA 89, 10336-10340

Scaria, P.V. & Schafer, R.H. (1996)
Calorimetric analysis of triple helices targeted to the d(G3A4G3).d(C3T4C3) duplex.
Biochemistry 35, 10985-10994

Semerad, C. L. & Maher, L. J. (1994)
Exclusion of RNA strands from a purine motif triple helix.
Nucleic Acids Res 22, 5321-5325

Shafer, R.H. (1998)
Stability and structure of model DNA triplexes and quadruplexes and their interactions with small ligands.
Progress in Nucleic Acid Research and Molecular Biology 59, 55-94.

Shimizu, M., Kubo, K., Matsumoto, U. & Shindo, H. (1993)
The loop sequence plays crucial roles for the isomerisation of intramolecular DNA triplexes in supercoiled plasmids.
J. Mol. Biol. 235, 185-197,

Shimizu, M., Inoue, H., Ohtsuka, E. (1994)
Detailed Study of Sequence-Specific DNA Cleavage of Triplex-Forming Oligonucleotides Linked to 1,10-Phenanthroline.
Biochemistry 33, 606-613

Sklenár, V. & Feigon, J. (1990)
Formation of a stable triplex from a single DNA strand.
Nature (London), 345, 836-838

Soyer, V.N. & Potaman, V.N. (1996)
Triple-helical nucleic acids.
Springer-Verlag New York, Inc.

Stilz, H.U. & Dervan, P.B. (1993)
Specific recognition of CG base pairs by 2-deoxynebularine within the purine-purine-pyrimidine triple-helix motif.
Biochemistry 32, 2177-2185

Ströbel, S.A., & Dervan, P.B. (1990)
Single-site enzymatic cleavage of yeast chromosome by oligonucleotide-directed triple-helix formation.
Science 249, 72-75

Sun, J.S., De Bizemont, T., Duval-Valentin, G., Thuong, N.T. & Hélène, C. (1991)
C. R. Acad. Sci III 3113, 585

Svinarchuck, F., Paoletti, J. & Malvy, C. (1995)
An unusually stable purine(purine-pyrimidine) short triplex.
J. Biol. Chem. 270, 14068-14071

Thielle, D. & Guschlbauer, W. (1968)
Evidence for a three stranded complex between poly I and poly C.
FEBS LETTERS 1, 173-175

Thielle, D. & Guschlbauer, W. (1969)
Protonated polynucleotides. VII. Thermal transitions between various polyinosinic, and polycytidylic acid complexes in acid media.
Biopolymers 8, 361-378
Thomas (1995)

Uhlmann, E. & Peyman, A. (1990)
Antisense oligonucleotides: a new therapeutic principle.
Chem. Rev. 90, 544-584

Van Meervelt, L., Vlieghe, D., Dautant, A., Galloia, B., Precigoux, G.
& Kennard, O. (1995)
High-resolution structure of a DNA helix forming (C.G)*G base triplets.
Nature 374, 742-744

Vary, C.P. (1992)
Triple-helical capture assay for quantitation of polymerase chain reaction products.
Cli. Chem. 38, 687-694

Vasquez, K.M., Wensel, T.G., Hogan, M.E., Wilson. J.H. (1995)
High-Affinity Triple Helix Formation by Synthetic Oligonucleotides at a site within a selectable mammalian gene.
Biochemistry 34, 7243-7251

Vo, T., Wang, S. & Kool, E.T. (1995)
Targeting pyrimidine single strands by triplex formation: structural optimisation of binding.
Nucleic Acids Research 23, 2937-2944

Völker, J. (1993)
The impact of local and global composition on the stability of triple helix formation.
PhD Thesis, University of Cape Town, South Africa.

Völker, J., Botes, D.P., Lindsey G.G. & Klump, H.H. (1993).
Energetics of a stable intramolecular DNA triple helix.
J. Mol. Biol. 230, 1278-1290.
JV-ITS d(5'-GAGAGAGAAACCCCTTTCTCTCTCTTTTCTCTCTCTTT-3')

Völker, J. & Klump, H.H. (1994). Electrostatic effects in DNA triple helices.
Biochemistry 33, 13502-13508.

Volkmann, S., Dannull, J. & Moeling, K. (1993)
The poly purine tract, PPT, of HIV as target for antisense and triple-helix-forming oligonucleotides.
Biochemistry 75, 71-78

Volkmann, S., Jendis, J., Frauendorf, A. & Moeling, K. (1995)
Inhibition of HIV-1 reverse transcription by triple-helix forming oligonucleotides with viral RNA
Nucleic Acids Research, 23, 12.4-1212

Wang, S., Booher, M.A. & Kool, E.T. (1994)
Stabilities of nucleotide loops bridging the pyrimidine strands in DNA pyrimidine-purine-pyrimidine triplexes: special stability of the CTTTG loop.
Biochemistry 33, 4639-4644

Wang, Z.Y., Lin, X.H., Nobuyoshi, M., Qui, Q.Q. & Deuel, T.F. (1992)
Binding of single-stranded oligonucleotides to a non B-form DNA structure results in loss of promoter activity of the platelet-derived growth factor A-chain gene.
J.Biol.Chem. 267, 13669-13674

Warner, R.C. (1957)
Studies on polynucleotides synthesised by polynucleotide phosporylase III. Interaction and ultraviolet absorption.
J. Biol. Chem. 229, 711-724

Washbrook, E. & Fox, K.R., (1994)
Comparison of antiparallel A.AT and T.AT triplets within an alternate strand DNA triple helix.
Nucleic Acids Research, 22, 3977-3982

Watson, J.D. & Crick, F.H.C. (1953).
Genetic implications of the structure of deoxyribonucleic acids.
Nature (London), 171, 964-967.

White, A.P. & Powell, J.W. (1995)
Observation of the hydration-dependent conformation of the $(dG)_{20}(dG)_{20}(dC)_{20}$ oligonucleotide triplex using FTIR Spectroscopy.
Biochemistry 34, 1137-1142

Xodo, L.E., Manzini, G. & Quadrifoglio, F (1990)
Spectroscopic and calorimetric investigation on the DNA triplex formed by d(CTCTTCTTTCTTTTCTTTCTTCTC) and d(GAGAAGAAAGA) at acidic pH.
Nucl. Acids Res. 18, 3557-3564

Xodo, L.E., Manzini, G. & Quadrifoglio, van der Marel, G. & van Boom, J. (1991)
Effect of 5-methylcytosine on the stability of triple stranded DNA-a thermodynamic study.
Nucl. Acids Res. 19, 5625-5631

Young, S.L., Krawczyk, S.H., Matteucci, M.D. & Toole, J.J. (1991)
Triple helix formation inhibits transcription elongation in vitro.
Proc. Nat. Acad. Sci. USA. 88, 100123-10026

Zamecnik, P.C. & Stephenson, M.L. 1978,
Inhibition of Rous sarcoma virus replication and cell transformation by a specific oligodeoxynucleotide.
Proc. Nat. Acad. Sci. USA. 75, 280-284

Appendix

6.1 Tertiary Education

1990-1992 Bachelor of Science (Biochemistry and Microbiology majors) UCT

1993 B.Sc.Hons. (Biochemistry, UCT); Supervisor: Prof. Horst H. Klump

1997 Internship (4th August to 22nd September)

Laboratoire de Biophysique (Director Mme. Dr. Thérèse Garestier)

Muséum National d'Histoire Naturelle (Director M. Henry de Lumley)

CNRS UA 481 INSERM U 201, 43 Rue Cuvier 75005, Paris

Supervisor: Dr. Jean-Louis Mergny (Tel: 0140793689)

6.2 Conferences Attended

1. "4th International Symposium on Applied Bioinorganic Chemistry (4IABC) with The Carman National Physical Chemistry Conference",
   The Forum, V & A Waterfront,
   Cape Town, 1-4 April 1997.

2. "Nucleic Acids and Related Macromolecules: Synthesis, Structure, Function and Applications" Ulm University, Germany, September 4-9, 1997.

3. "Year of Science and Technology Exhibition," V & A Waterfront, Cape Town, March, 1998

6.3 Publications

1. "Triple helical structures involving inosine: There is a penalty for promiscuity."

   Mills, M., Völker, J. & Klump, H. (1996)

   Biochemistry 35, 13338-13344

2. "A new twist to an old tale: The influence of the exchange of thymine for adenine on the stability of a purine motif DNA triple helix."

   Mills, M. & Klump, H.H. (1997)

   South African Journal of Chemistry 50(4), 184-188

3. "Systematic mutation in the third strand of a purine motif DNA triple helix: A story of a molecule which hides it's tail."

   Mills, M. & Klump, H.H. (1998)

   Nucleotides and Nucleosides (in press)

FINIS.